Identification of PIMREG as a novel prognostic signature in breast cancer via integrated bioinformatics analysis and experimental validation

Wenjing Zhao[1,*], Yuanjin Chang[2,*], Zhaoye Wu[2], Xiaofan Jiang[2], Yong Li[1], Ruijin Xie[2], Deyuan Fu[1], Chenyu Sun[3,4] and Ju Gao[1]

[1] Clinical Medical College, Yangzhou University, Yangzhou, Jiangsu, China
[2] School of Medicine, Jiangnan College, WuXi, JiangSu, China
[3] Department of General Surgery, The second Affiliated Hospital of Anhui Medical University, Anhui, China
[4] Department of Medicine, AMITA Health Saint Joseph Hospital, Chicago, IL, USA
[*] These authors contributed equally to this work.

ABSTRACT

Background. Phosphatidylinositol binding clathrin assembly protein interacting mitotic regulator (PIMREG) expression is upregulated in a variety of cancers. However, its potential role in breast cancer (BC) remains uncertain.

Methods. The Cancer Genome Atlas (TCGA) and Gene Expression Omnibus (GEO) databases were used to gather relevant information. The expression of PIMREG and its clinical implication in BC were assessed by using Wilcoxon rank-sum test. The prognostic value of PIMREG in BC was evaluated through the Cox regression model and nomogram, and visualized by Kaplan-Meier survival curves. Genes/proteins that interact with PIMREG in BC were also identified through GeneMANIA and MaxLink. Gene set enrichment analysis (GSEA) was then performed. The correlations of the immune cell infiltration and immune checkpoints with the expression of PIMREG in BC were explored via TIMER, TISIDB, and GEPIA. Potential drugs that interact with PIMREG in BC were explored via Q-omic. The siRNA transfection, CCK-8, and transwell migration assay were conducted to explore the function of PIMREG in cell proliferation and migration.

Results. PIMREG expression was significantly higher in infiltrating ductal carcinoma, estrogen receptor negative BC, and progestin receptor negative BC. High expression of PIMREG was associated with poor overall survival, disease-specific survival, and progression-free interval. A nomogram based on PIMREG was developed with a satisfactory prognostic value. PIMREG also had a high diagnostic ability, with an area under the curve of 0.940. Its correlations with several immunomodulators were also observed. Immune checkpoint CTLA-4 was significantly positively associated with PIMREG. HDAC2 was found as a potentially critical link between PIMREG and BRCA1/2. In addition, PIMREG knockdown could inhibit cell proliferation and migration in BC.

Conclusions. The high expression of PIMREG is associated with poor prognosis and immune checkpoints in BC. HDAC2 may be a critical link between PIMREG and BRCA1/2, potentially a therapeutic target.

INTRODUCTION

Breast cancer (BC) is the most commonly diagnosed malignant tumor among females worldwide. It is the leading cause of cancer-related fatalities, accounting for 6.9% of all cancer diagnoses (*Breastcancer.org, 2023*). It imposes substantial disease and economic burdens on both developed and developing countries (*Najafi et al., 2019*; *Sung et al., 2021*). Despite the fact that early BC screening and identification are critical for reducing morbidity and mortality by locoregional surgery, conventional chemotherapy, and radiotherapy, the recurrence rate of BC remains high, leading to an elevated risk of death. (*Hamann et al., 2019*; *Mayor, 2015*). The prediction of clinical prognosis in BC largely depends on our understanding of the clinical, pathological, and molecular characteristics of BC. Still, the underlying etiology of BC aggressiveness is yet unknown. Identifying potential diagnostic and prognostic biomarkers of BC would help both detect BC patients and understand BC etiology (*Arnedos et al., 2019*; *Duffy et al., 2015*).

Phosphatidylinositol binding clathrin assembly protein interacting mitotic regulator (PIMREG), also known as FAM64A, was discovered to be a clathrin assembly lymphoid myeloid leukemia gene (CALM) interactor. It is located at 17p13.2 and plays the key role in modulating the subcellular localization of the leukemogenic fusion protein CALM/AF10 (*Archangelo et al., 2008*). It has been shown that PIMREG controls the transition from metaphase to anaphase of the cell's mitotic cycle, so it could be a marker for the proliferation and tumorigenesis of various cancer kinds (*Barbutti et al., 2016*; *Zhao et al., 2008*). Recent studies revealed that PIMREG is upregulated in many different types of cancer, such as prostate cancer, lung cancer, gastric cancer, esophageal cancer, colorectal cancer, and most importantly, BC (*Jiang et al., 2021*; *Zhou et al., 2021*; *Zhu et al., 2021*). Also, elevated PIMREG expression is associated with a worse prognosis among patients with lung, liver, pancreatic, and other types of cancer. However, the underlying mechanism of PIMREG in BC, its prognostic value in different types of BC, and its diagnostic value in BC are yet to be further explored. Moreover, the previous research indicated that PIMREG overexpression significantly activates NF-κB signaling and promotes breast cancer aggressiveness, and the immune infiltrates associated with the upregulation of PIMREG in BC require further investigation (*Jiang et al., 2019*), and potential therapies targeted to PIMREG in BC need to be developed.

In this study, we combined bioinformatics analysis and cell biology experiments to investigate the roles and clinical values of PIMREG in BC. We first explored the prognostic and diagnostic significance of PIMREG using data extracted from the Cancer Genome Atlas (TCGA) database. Then, we investigated the role of PIMREG in BC pathogenesis through Gene set enrichment analysis (GSEA) and network analysis. Furthermore, we examined the correlation of PIMREG with immune checkpoints and the level of immune infiltration. We also explored drugs that potentially respond to overexpression of PIMREG in BC, as they might offer novel immunological perspectives to understand the mechanism of tumor

progression and provide useful evidence for future studies regarding the immunological and pharmacological therapies for BC patients. Finally, experimental validation was conducted to verify the expression of PIMREG in BC and explore its function on cell proliferation and migration in BC. This study aimed to identify a prognostic signature and provide future cancer therapeutics in breast cancer.

METHODS

Analysis of PIMREG expression level

The gene expression data of 1109 BC tissues and 113 adjacent normal tissues were obtained from the Breast Invasive Carcinoma Project (TCGA-BRCA) of the TCGA database. The clinicopathological characteristics of the patient's data were summarized. Wilcoxon rank-sum test was used to assess the expression level of PIMREG between BC and adjacent normal tissue; visualization was performed using the 'ggplot2' package in R software v3.6.3 (*R Core Team, 2020*; *Ding et al., 2022*). Further analysis was conducted on information obtained from 112 pairs of breast cancer tissue samples and adjacent normal breast tissues. Moreover, subgroup analyses were conducted based on T, N, M stage, pathologic stage, PR status, HER-2 status, and ER status. Statistical significance was considered when p <0.05. Findings were verified through the GSE42568 data set, which including104 BC tissues and 17 normal tissues. Data obtained from Gene Expression Omnibus (GEO) database set aimed to analyze the expression difference of PIMREG between BC tissues and normal breast tissue (*Clarke et al., 2013*; *Zhou et al., 2020*). All figures were visualized using the R package ggplot2. To evaluate and verify the expression of PIMREG in BC, images of immunohistochemical (IHC) staining for the PIMREG protein obtained from the Human Protein Atlas (HPA) (http://www.proteinatlas.org/) were used (*Pontén et al., 2011*; *Zhu et al., 2022*).

Prognosis analysis of PIMREG expression within BC

Using RNAseq data with Log2 transformed TPM (transcripts per million reads) of TCGA-BRCA, the prognostic significance of PIMREG expression was first investigated. To compare the survival difference, as well as overall survival (OS), disease-specific survival (DSS), and progression-free interval (PFI), between high PIMREG and low PIMREG expression groups, we applied the Kaplan–Meier (KM) survival analysis with the log-rank test. Log-rank tests and univariate Cox proportional-hazards regression were performed to create the KM curves, which included *p*-values and hazard ratio (HR) with a 95% confidence interval (CI). The KM curve of OS based on the GEO database (GSE42568) was also plotted with the same method. R software with 'survminer' and 'survival' packages was used to perform these calculations. Furthermore, using the "plotROC" package, the diagnostic property was verified through receiver operating characteristic (ROC) analysis of BC. Meanwhile, in order to explore and further clarify the risk factors in patients with BC, the univariate analysis of the correlation between clinicopathological characteristics and OS in BC was also performed. A forest plot was developed to visualize these univariate and multivariate analyses. Based on overexpressed PIMREG and other potential predictors, a predictive model based on TCGA-BRCA data was also developed to predict the mortality

risk (*Balachandran et al., 2015*; *Iasonos et al., 2008*; *Liu et al., 2018*). A nomogram using 'rms' and 'survival' R packages was constructed to create a graphical representation of potential predicting factors for calculating mortality risk for an individual patient and predicting the 1-, 3-, and 5-year overall survival. All figures were visualized using the R package 'ggplot2'.

GSEA

Based on transcriptional sequences obtained from TCGA, GSEA was used to identify gene sets and pathways associated with PIMREG. Gene expressions were classified into high-expression and low-expression groups. To assess the potential functions of these groups, we conducted a comparative analysis using GSEA *via* the Broad Institute website (https://www.gsea-msigdb.org/gsea/index.jsp), utilizing the R package cluster profiler (*Subramanian et al., 2005*; *Yu et al., 2012*). The results of this analysis were visually presented using the R package 'ggplot2'.

Explore other genes/proteins that interacted with PIMREG

The protein-protein interaction (PPI) networks of the PIMREG were constructed *via* GeneMANIA (http://www.genemania.org) (*Vlasblom et al., 2015*). In addition, the MaxLink web server (https://funcoup5.scilifelab.se/maxlink/) was conducted to find and rank other cancer gene candidates by their connectivity to the PIMREG and the two most commonly expressed genes for BC, *i.e.,* BRCA1 and BRCA2 (*Guala, Sjölund & Sonnhammer, 2014*).

Infiltration of immune cells

We utilized TIMER2.0, a web-based tool for comprehensive molecular characterization of tumor-immune interactions, to examine the infiltration of different immune cells and their clinical effects (*Li et al., 2017*). Using the Gene module in TIMER2.0, we created plots to explore the correlation between the expression of PIMREG members and immune infiltration level in BC. A significant correlation is set for the cutoff value of Cor >0.2 and p<0.05 (*Li et al., 2016*; *Liu et al., 2021*; *Zhong et al., 2021*).

To investigate interactions and relationships between the immune system and PIMREG, we employed the TISIDB database (http://cis.hku.hk/TISIDB). TISIDB is an online platform for evaluating immune system and tumor interactions, including almost 1,000 reported immune-related anti-tumor genes, etc., and immunological data aggregated from seven public databases (*Ding et al., 2021*; *He et al., 2021*; *Xu et al., 2021*). This study used TISIDB to explore highly associated immunomodulators with PIMREG in BC.

Relationship between PIMREG and immune checkpoints in BC

To investigate the potential oncogenic role of PIMREG in breast cancer (BC), we assessed its associations with immune checkpoints using TIMER and GEPIA. In this study, we focused on the immune checkpoints programmed death 1 (PD1)/PD1-L1 and cytotoxic T-lymphocyte-associated protein 4 (CTLA-4) as they are well-recognized critical checkpoints in tumor immune evasion (*De Velasco et al., 2017*; *Li et al., 2017*; *Lou et al., 2021*; *Xu et al., 2018*).

Table 1 Clinical information of patients involved in this study.

Variables	
No of patients	5
Age (years, mean)	49.2 ± 12.498
Sex (%)	
Female	5 (100%)
Male	0
Tumor size	
≤ 2.0 cm	1 (20%)
>2.0 cm	4 (80%)
Lymph node metastasis (%)	
Yes	3 (60%)
No	2 (40%)
Menopause (%)	
Yes	3 (60%)
No	2 (40%)
Stage/grade (%)	
I~II	3 (60%)
III~IV	2 (40%)
Unknown	0

Investigate potential drugs that demonstrate interaction with PIMREG in BC

Q-omics (version 1.0) was employed to investigate drugs that exhibit a potentially favorable response to PIMREG. The score, developed by Q-omics, represents the log-fold change in drug response between samples with high PIMREG expression and those with low PIMREG expression. This scoring system was utilized to identify drugs demonstrating the strongest response to high PIMREG expression (*Jeong et al., 2020*; *Lee et al., 2021*).

Human tissue samples collection

We collected five surgically removed breast cancer (BC) tissues and their matched adjacent normal tissues from Northern Jiangsu People's Hospital, affiliated with Yangzhou University, between October 2022 and February 2023. The clinical information of the patients is provided in Table 1. All participants in this study provided written informed consent, and the study protocol was approved by the ethics committee of Northern Jiangsu People's Hospital, affiliated with Yangzhou University (Approval ID: 2022KY316).

Cell lines

The human mammary epithelial cell line MCF-10A (#CL-0525) and the human breast cancer cell line MDA-MB-231 (#CL-0150B) were obtained from Procell (Wuhan, China). MCF-10A cells were cultured in DMEM/F12 (Gibco, CA, USA) supplemented with 5% horse serum, 0.5 μg/ml hydrocortisone, 20 ng/ml human epidermal growth factor, 10 μg/ml insulin, and 1% penicillin/streptomycin. MDA-MB-231 cells were cultured in Dulbecco's modified Eagle's medium (DMEM, Hyclone, UT, USA), supplemented with

10% fetal bovine serum and 1% penicillin/streptomycin. Before further experiments, these cells were incubated in a humidified atmosphere containing 5% CO$_2$ at 37 °C.

Quantitative real-time reverse transcription PCR (qRT-PCR)

To assess the mRNA levels in cells, quantitative real-time polymerase chain reaction (qRT-PCR) was performed following a previously published protocol (*Xie et al., 2022*). Total RNA was extracted from the cells using the TRizol reagent (Takara, Shiga, Japan). Subsequently, the PrimeScriptTM RT reagent kit (Takara, Shiga, Japan) was utilized to synthesize single-stranded cDNA from the RNA, following the manufacturer's instructions. The 2 $-\Delta\Delta$Ct value method, which involves determining the cycle at which the fluorescence level reaches the threshold limit set by the qPCR system, was employed to calculate the relative gene expression in the target and reference samples (*Rao et al., 2013*). This study used it to calculate the relative mRNA expression of PIMREG or HDAC2. Glyceraldehyde 3-phosphate dehydrogenase (GAPDH) was used as an endogenous control. The sequences of RT-PCR primers were used as follows: PIMREG: forward 5′-CCTGGAAACGCCTGGAAAC-3′and reverse 5′-CAAAGCACTCTTAGCTGAGCG-3'; HDAC2: forward 5'- ATGGCGTACAGTCAAGGAGG-3' and reverse 5'-TGCGGATTCTATGAGGCTTCA-3'; GAPDH: forward 5′-ATTCCACCCATGGCAAATTC-3′and reverse 5′-TGGGATTTCCATTGATGACAAG.

Western blot assay

To examine the protein expression of PIMREG in cells and BC tissues, a western blot assay was performed based on a previously published protocol (*Xie et al., 2022*). Briefly, the cells or BC tissues were lysed using RIPA reagent (Beyotime, Shanghai, China) and boiled for 10 min. Subsequently, the total proteins were separated by 10% sodium dodecyl sulfate-polyacrylamide gel electrophoresis (SDS-PAGE) and transferred onto PVDF membranes (Millipore, Billerica, MA, USA). The membranes were then blocked with 5% nonfat milk diluted with Tris-buffered saline-Tween (TBST) at room temperature for 1 h and incubated overnight at 4 °C with the primary antibody: anti-PIMREG (1:500; abs152589; Absin Bioscience, Inc., Shanghai, China). The next day, the membranes were incubated with the HRP-conjugated secondary antibodies at room temperature for 1 h. The Western blots were visualized using an ECL detection kit (Proteintech Group, Inc., Rosemont, IL, USA) for chemiluminescence. The density of the protein bands was quantified using Image J software (Pierce, Rockford, IL, USA), and the values was normalized to β-Actin.

Immunohistochemistry assay

The immunohistochemistry (IHC) assay followed a previously published protocol (*Jin et al., 2018*). Briefly, paraffin-embedded breast tissue slides with a thickness of 5 μm were incubated overnight at 4 °C with anti-PIMREG (1:50; abs152589; absin, Shanghai, China). Subsequently, the slides were incubated with the secondary antibody at room temperature for 1 h. Then, the slides were incubated in diaminobenzidine (DAB) and counterstained with hematoxylin. Images of the slides were captured under a microscope.

Transfection assay

To knockdown the expression of the PIMREG, the siRNA transfection assay was conducted based on the previously published paper (*Yao et al., 2019*). Briefly, cells were seeded into a 6-well plate and transfected with Lipo8000™ Transfection Reagent (#C0533, Beyotime, Shanghai, China) following the manufacturer's instructions. After 48 h of siRNA transfection, the knockdown efficiency was confirmed by conducting a western blot assay or qRT-PCR. The siRNA targeting human PIMREG or HDAC2 mRNA was designed by Genepharma Technologies Inc (Shanghai, China), and the siRNA sequences were used as follows: siPIMREG: 5′-UCCUGGAAACGCCUGGAAATT-3′, si-HDAC2: 5′-GGAUUACAUCAUGCU AAGA-3′.

Colony formation assay

To investigate the impact of HDAC2 on breast cancer, a colony formation assay was performed following a previously published protocol (*Kim & Ma, 2018*). Briefly, MDA-MB-231 cells were transfected with si-HDAC2 and subsequently seeded in 6-well plates at a density of 1000 cells per well. The cells were then incubated for 7 days to allow colony formation. Afterward, the colonies were fixed with 4% paraformaldehyde for 30 min and stained with 0.5% crystal violet for 30 min. The number of colonies was quantified using ImageJ software.

Cell counting kit-8 (CCK-8) assay

To assess the cell proliferation of MDA-MB-231 cells transfected with siRNA-PIMREG, a CCK-8 assay was performed following a previously published protocol (*Xie et al., 2022*). Briefly, after transfection with siRNA-PIMREG, MDA-MB-231 cells were seeded in 96-well plates at a volume of 100 μL/well, with 5000 cells per well. The cells were then incubated for 0 h, 24 h, 48 h, and 72 h. Subsequently, 10 μL of CCK8 solution (Beyotime, Shanghai, China) was added to each well, and the plate was further incubated for 30 min. Finally, the cell proliferation was measured by recording the absorbance at 450 nm using a microplate reader.

Transwell migration assay

To assess the migration ability of cells transfected with siRNA-PIMREG, a transwell migration assay was conducted following a previously published protocol (*Yao et al., 2019*). Briefly, after transfection with siRNA-PIMREG, 5×10^4 cells were seeded in the upper chamber with an 8 μm pore size (Corning Costar). The lower chamber was filled with DMEM containing 10% FBS to stimulate cell migration. After incubation for 12 h, the migrated cells were fixed with 4% paraformaldehyde for 30 min and stained with 0.1% crystal violet for 30 min. Images of the migrated cells were captured under a microscope.

Statistical analysis

The bioinformatics analysis in this study was conducted using the online database mentioned above or the R software. The experimental results are presented as mean $\pm$ standard deviation (SD), and the differences between the two groups were compared using the Student's t-test. Each experiment was repeated three times. Statistical significance was defined as a P value <0.05 or a log-rank P value <0.05.

RESULTS

Correlation analysis of PIMREG expressions in BC

Among the data downloaded from TCGA, a total of 1109 samples were available. However, the demographic and clinical data were only accessible for 1083 patients with breast cancer (Table 2). The analysis revealed significant associations between the expression of PIMREG and various clinicopathological parameters. These parameters include race ($P < 0.001$), T stage ($P < 0.001$), pathologic stage ($P = 0.002$), histological type ($P < 0.001$), PR status ($P < 0.001$), ER status ($P < 0.001$), and PAM50 status ($P < 0.001$) in breast cancer patients. These findings suggest that PIMREG may serve as a promising novel biomarker in the context of breast cancer.

Upregulation of PIMREG in BC

The analysis of mRNA expression data from the TCGA database revealed a significantly higher average expression level of PIMREG in BC tissues compared to normal tissues ($P < 0.001$) (Fig. 1A). This finding was further confirmed by analyzing matched tumors and surrounding samples, which demonstrated higher expression of PIMREG in BC tumor tissues (Fig. 1B). Consistent results were obtained from the expression difference analysis based on the GEO database ($P < 0.001$) (Fig. 1C). Subsequent analysis showed a significant difference in PIMREG expression between pathologic stage I and stage II, with higher expression observed in stage II ($P < 0.001$) (Fig. 2A). Moreover, more advanced T stage was associated with higher expression of PIMREG ($P < 0.001$) (Fig. 2B). However, there was no association between the M and N stages with PIMREG expression (Figs. 2C–2D). Regarding hormone receptor status, PIMREG expression was found to be elevated in estrogen receptor (ER) negative BC tissues compared to ER-positive tissues, and it was even more increased in progestin receptor (PR) negative BC tissues compared to PR-positive tissues ($P < 0.001$) (Figs. 2E–2F). However, no statistically significant difference was observed between human epidermal growth factor receptor 2 (HER2) positive and HER2-negative BC tissues (Fig. 2G). Additionally, PIMREG expression was significantly higher in infiltrating ductal carcinoma compared to infiltrating lobular carcinoma ($P < 0.001$) (Fig. 2H). To further support these findings, immunohistochemistry (IHC) images obtained from datasets of the Human Protein Atlas (HPA) were used to demonstrate PIMREG protein expression in BC and breast tissues. The intensity of PIMREG staining was weak in normal breast tissue but moderate in BC tissues, confirming the elevated expression of PIMREG in BC compared to normal breast tissue (Fig. 3). Overall, these results indicate that PIMREG is likely overexpressed in breast cancer.

Prognostic property of PIMREG in BC

The TCGA database was used to assess the impact of the upregulation of PIMREG on BC prognosis. Its upregulation was revealed to be associated with worse OS (HR: 1.48; 95%CI [1.17–2.03]; $P = 0.018$) and DSS (HR: 1.78; 95%CI [1.15–2.76]; $P = 0.009$), as well as shorter PFI (HR: 1.64; 95%CI [1.18–2.28]; $P = 0.003$) in patients with BC (Figs. 4A–4C). In addition, receiver operating characteristic (ROC) analysis was also performed with an area under the curve (AUC) value of 0.940 (95%CI [0.919–0.961]), indicating a high

Table 2 Correlation between PIMREG and clinicopathological characteristics from TCGA-BRCA dataset.

Characteristic	Low expression of PIMREG	High expression of PIMREG	p
n	541	542	
T stage, n (%)			<0.001
T1	167 (15.5%)	110 (10.2%)	
T2	283 (26.2%)	346 (32%)	
T3	75 (6.9%)	64 (5.9%)	
T4	15 (1.4%)	20 (1.9%)	
N stage, n (%)			0.135
N0	259 (24.3%)	255 (24%)	
N1	171 (16.1%)	187 (17.6%)	
N2	54 (5.1%)	62 (5.8%)	
N3	47 (4.4%)	29 (2.7%)	
M stage, n (%)			0.293
M0	446 (48.4%)	456 (49.5%)	
M1	7 (0.8%)	13 (1.4%)	
Pathologic stage, n (%)			0.002
Stage I	109 (10.3%)	72 (6.8%)	
Stage II	283 (26.7%)	336 (31.7%)	
Stage III	131 (12.4%)	111 (10.5%)	
Stage IV	7 (0.7%)	11 (1%)	
Race, n (%)			<0.001
Asian	24 (2.4%)	36 (3.6%)	
Black or African American	59 (5.9%)	122 (12.3%)	
White	420 (42.3%)	333 (33.5%)	
Age, n (%)			0.030
<=60	282 (26%)	319 (29.5%)	
>60	259 (23.9%)	223 (20.6%)	
Histological type, n (%)			<0.001
Infiltrating Ductal Carcinoma	335 (34.3%)	437 (44.7%)	
Infiltrating Lobular Carcinoma	152 (15.6%)	53 (5.4%)	
PR status, n (%)			<0.001
Negative	102 (9.9%)	240 (23.2%)	
Indeterminate	2 (0.2%)	2 (0.2%)	
Positive	412 (39.8%)	276 (26.7%)	
ER status, n (%)			<0.001
Negative	50 (4.8%)	190 (18.4%)	
Indeterminate	0 (0%)	2 (0.2%)	
Positive	466 (45%)	327 (31.6%)	
HER2 status, n (%)			0.550
Negative	287 (39.5%)	271 (37.3%)	
Indeterminate	7 (1%)	5 (0.7%)	
Positive	74 (10.2%)	83 (11.4%)	

Table 2 (*continued*)

Characteristic	Low expression of PIMREG	High expression of PIMREG	p
Menopause status, n (%)			0.709
Pre	119 (12.2%)	110 (11.3%)	
Peri	18 (1.9%)	22 (2.3%)	
Post	354 (36.4%)	349 (35.9%)	
PAM50, n (%)			<0.001
Normal	31 (2.9%)	9 (0.8%)	
Luminal A	416 (38.4%)	146 (13.5%)	
Luminal B	55 (5.1%)	149 (13.8%)	
Her2	28 (2.6%)	54 (5%)	
Basal	11 (1%)	184 (17%)	
Anatomic neoplasm subdivisions, n (%)			0.412
Left	274 (25.3%)	289 (26.7%)	
Right	267 (24.7%)	253 (23.4%)	
radiation therapy, n (%)			0.501
No	230 (23.3%)	204 (20.7%)	
Yes	280 (28.4%)	273 (27.7%)	
Age, median (IQR)	60 (49, 68)	57 (48, 66.75)	0.085
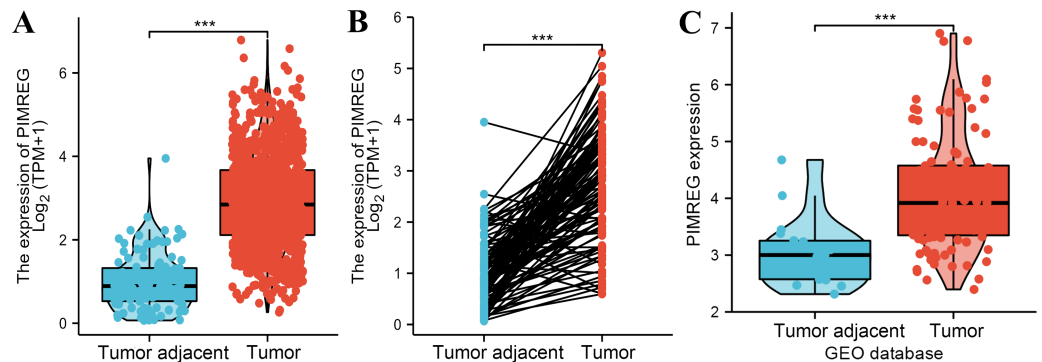
Figure 1 **The level of PIMREG expression in breast cancer tissue *vs* normal tissues (sample size = 1109 from TCGA database, 104 from GEO database).** (A) Comparison of expression level of PIMREG between breast tissues and normal breast sample based on TCGA database. (B) The expression level of PIMREG in normal breast sample and matched breast cancer tissues based on TCGA. (C) Comparison of expression level of PIMREG between samples from breast cancer and samples from normal breast based on GEO database (GSE42568). Asterisks (***) indicate $p < 0.001$.

Full-size 🖼 DOI: 10.7717/peerj.15703/fig-1

prognostic value of PIMREG (Fig. 4D). Further analysis of subgroups found that the upregulation of PIMREG was associated with worse OS in infiltrating lobular carcinoma with HR of 2.79 (95%CI [1.13–6.75]; $P = 0.026$), but not in infiltrating ductal carcinoma. (Figs. 5A–5B) Based on the GEO database, the higher expression of PIMREG was also found to be associated with worse OS in BC (HR: 2.28; 95%CI [1.13–4.59]; $P = 0.021$). (Fig. 5C) As PAM50 classifies BC into five molecular intrinsic subtypes that differ in their
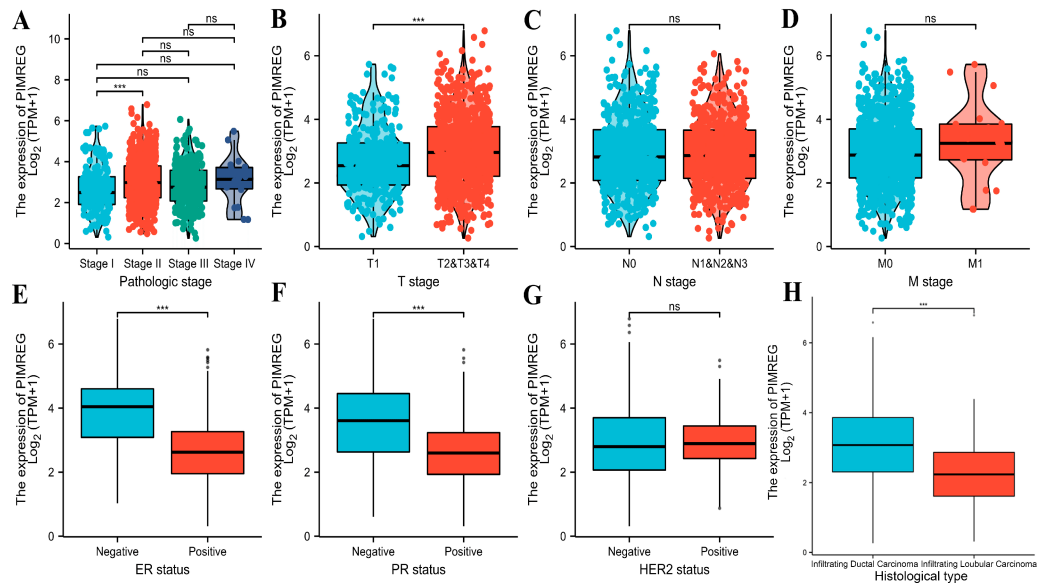
Figure 2 **Correlation between the expression of PIMREG and certain clinicopathological factors (sample size = 1109 from TCGA database).** (A) Clinical stage. (B) T classification. (C) N classification. (D) M classification. (E) ER status. (F) PR status. (G) HER2 status. (H) histology type. Asterisks (***) indicate $p < 0.001$; ns indicates non-significant ($p > 0.05$).
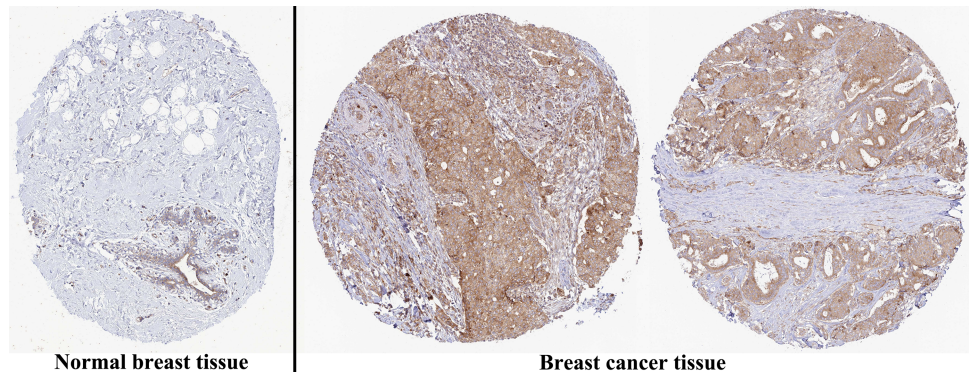
Full-size 🖼 DOI: 10.7717/peerj.15703/fig-2

Figure 3 **Representative images of immunohistochemical staining of normal breast (left panels) and breast cancer (right panels, Lobular carcinoma (F), Duct carcinoma (R)) from Human Atlas.** Tissue slides were incubated with anti-PIMREG (1:150; HPA043783; Sigma Aldrich, St. Louis, MO, USA) at 4 °C, and the PIMREG protein level was increased in breast cancer tissue.

Full-size 🖼 DOI: 10.7717/peerj.15703/fig-3

biological properties and prognoses, a subgroup analysis based on PAM50 subtypes was also performed, but did not indicate statistical significance (Fig. 6).

To further explore and identify the risk factors in patients with BC, a univariate Cox proportional-hazards regression analysis was conducted. The results showed that T stage, M stage, N stage, pathologic stage, age, and menopause status were associated with worse OS ($P = 0.046$, $P < 0.001$, $P < 0.001$, $P = 0.003$, $P < 0.001$, and $P = 0.003$, respectively)
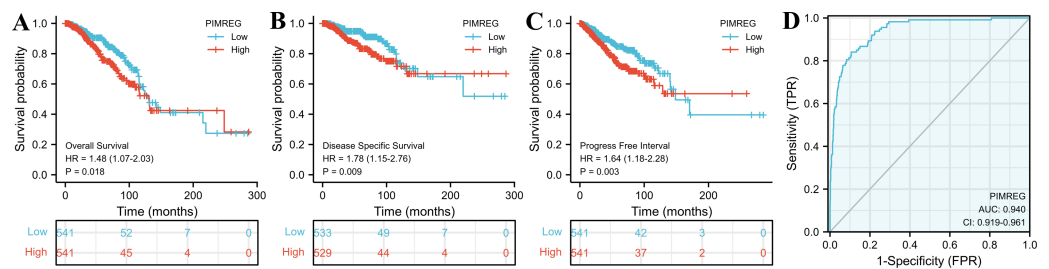
Figure 4 **The outcomes of breast cancer in high PIMREG expression and low PIMREG expression groups (sample size = 1109 from the TCGA database).** (A) Overall survival (OS). (B) Disease-specific survival (DSS). (C) Progression-free interval (PFI). (D) The receiver operating characteristic curve (ROC).
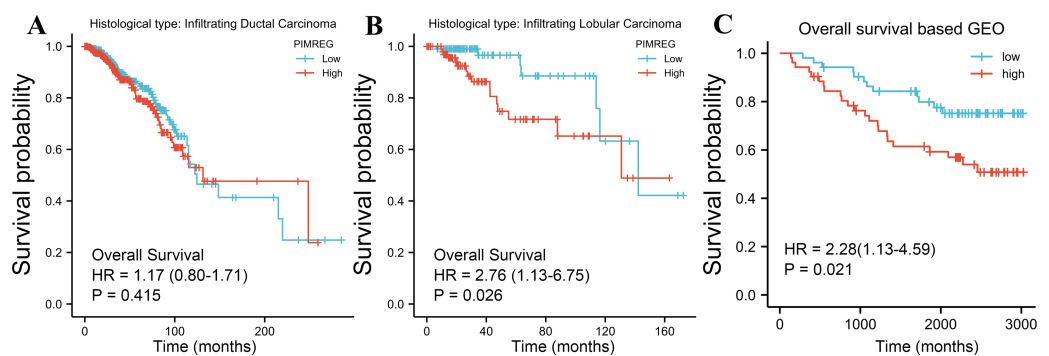Full-size ☒ DOI: 10.7717/peerj.15703/fig-4

Figure 5 **Subgroup overall survival (OS) analysis based on the low and high expression of PIMREG (sample size = 1109 from the TCGA database, 104 from the GEO database).** (A) Infiltrating ductal carcinoma. (B) Infiltrating lobular carcinoma. (C) OS based on the GEO database (GSE42568).
Full-size ☒ DOI: 10.7717/peerj.15703/fig-5

(Fig. 7). In addition, the higher expression of PIMREG was detected (HR = 1.475, 95%CI [1.070–2.034], $P = 0.018$) and was determined to be a significant predictor of worse OS.

The above results suggested that the T stage, N stage, M stage, age, pathologic stage, and menopause status might be linked to prognosis. As the pathologic stage of breast cancer is based on the TNM stage system, thus only the TNM stage was applied here for nomogram development. Therefore, a prognostic nomogram based on TNM stage, age, menopause, and PIMREG expression level was developed to predict individual survival probability (Fig. 8A). The C index of the nomogram was $0.741(0.713 - 0.769)$, indicating its potential for the prediction of overall survival. The calibration curve of this prediction model showed that the established lines of 1-, 3- and 5-year survival matched the ideal line at a relatively high degree (Fig. 8B). Collectively, these results indicated that PIMREG may be a prognostic signature for BC.

Identities in PIMREG-related signaling pathway identified by GSEA

GSEA was conducted to identify the differences in signaling pathways between low- and high-PIMREG expression datasets (Fig. 9). The result revealed that PIMREG was related to
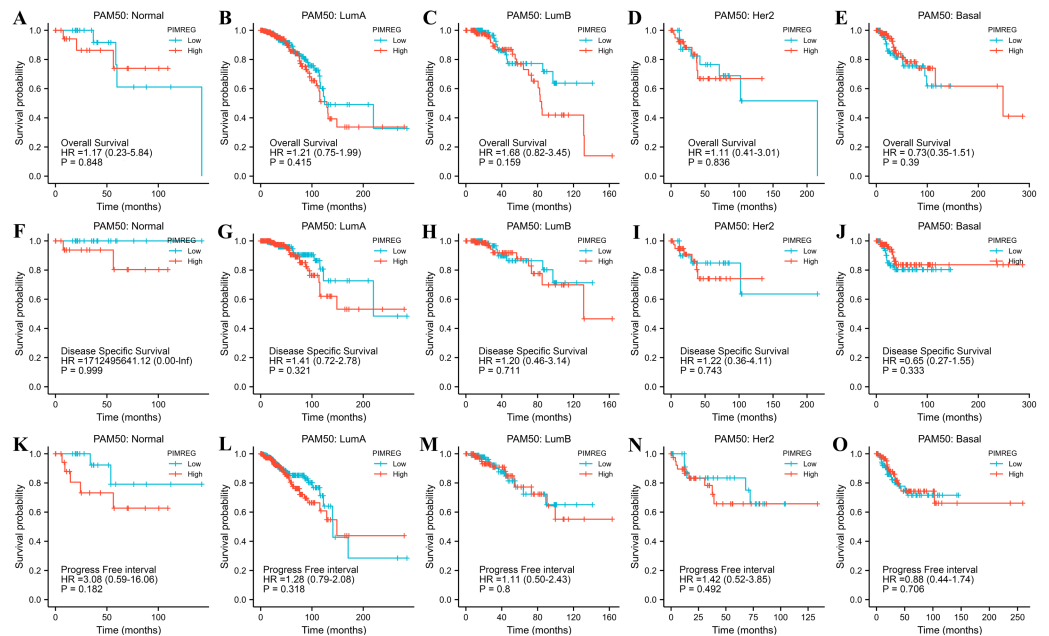
Figure 6 **The outcomes of breast cancer in high PIMREG expression and low PIMREG expression groups based on PAM50 subtypes (sample size = 1109 from TCGA database).** (A) Overall survival (OS) of Normal-like subtype, (B) OS of Luminal A subtype, (C) OS of Luminal B subtype, (D) OS of HER2-enriched subtype, (E) OS of Basal-like subtype, (F) Disease-specific survival (DSS) of Normal-like subtype, (G) DSS of Luminal A subtype, (H) DSS of Luminal B subtype, (I) DSS of HER2-enriched subtype, (J) DSS of Basal-like subtype, (K) Progression-free interval (PFI) of Normal-like subtype, (L) PFI of Luminal A subtype, (M) PFI of Luminal B subtype, (N) PFI of HER2-enriched subtype, (O) PFI of Basal-like subtype.

Full-size 🖼 DOI: 10.7717/peerj.15703/fig-6

the neuroactive ligand–receptor interaction, NABA-secreted factors, cell cycle checkpoint, Class A1 Rohdopsin-like receptor, DNA repair, mRNA splicing, and translation pathways.

Immune cell infiltration of PIMREG in BC

The relationship between PIMREG and immune cell infiltration was studied using the TIMER database, as immune cell levels often correspond to cancer cell proliferation and progression (Fig. 10) (*Grenier, Yeung & Khanna, 2018*). A statistically significant correlation was found between PIMREG expression and the infiltration of macrophages, neutrophils, and dendritic cells. However, the correlation coefficients did not quite reach conventional levels of a positive Spearman's rho value (<0.3).

To further explore the association between PIMREG and immunomodulators, three immunoinhibitors that were most correlated with PIMREG were Lymphocyte Activating 3 (LAG3), Indoleamine 2,3-dioxygenase 1 (IDO1), and CTLA-4 (Figs. 11A–11C). On the other hand, the three immunostimulators that showed the strongest correlation with PIMREG were poliovirus receptor (PVR), human UL16-binding protein 1 (ULBP1), and tumor necrosis factor (TNF)-receptor superfamily 13C (TNFRSF13C) (Figs. 11D–11F).

Regarding major histocompatibility complex (MHC) molecules, transporter associated with antigen processing 2 (TAP2), transporter associated with antigen processing 1 (TAP1),
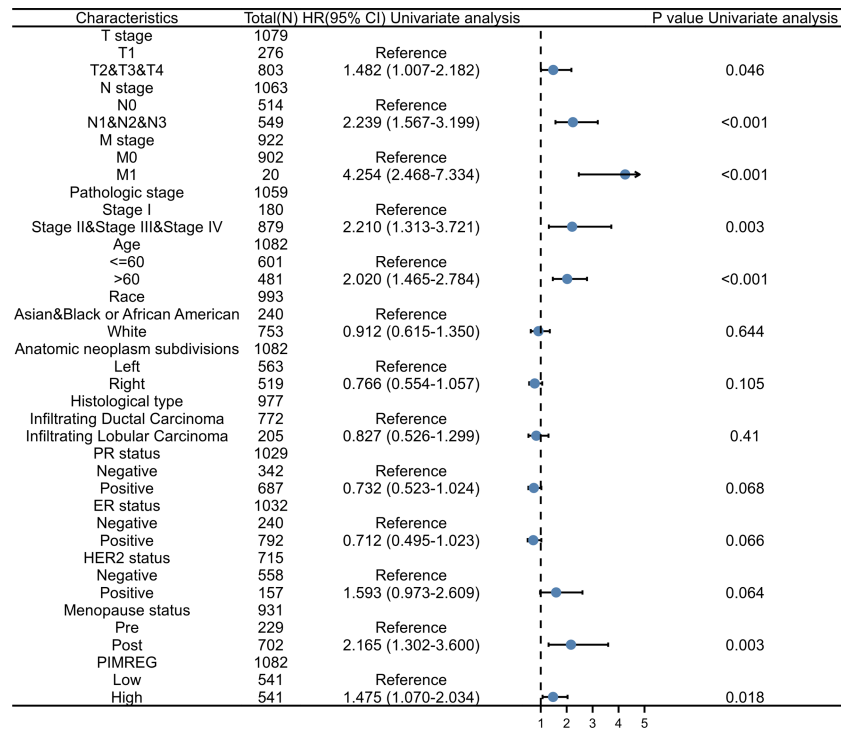
Characteristics	Total(N)	HR(95% CI) Univariate analysis		P value Univariate analysis
T stage	1079			
T1	276	Reference		
T2&T3&T4	803	1.482 (1.007-2.182)		0.046
N stage	1063			
N0	514	Reference		
N1&N2&N3	549	2.239 (1.567-3.199)		<0.001
M stage	922			
M0	902	Reference		
M1	20	4.254 (2.468-7.334)		<0.001
Pathologic stage	1059			
Stage I	180	Reference		
Stage II&Stage III&Stage IV	879	2.210 (1.313-3.721)		0.003
Age	1082			
<=60	601	Reference		
>60	481	2.020 (1.465-2.784)		<0.001
Race	993			
Asian&Black or African American	240	Reference		
White	753	0.912 (0.615-1.350)		0.644
Anatomic neoplasm subdivisions	1082			
Left	563	Reference		
Right	519	0.766 (0.554-1.057)		0.105
Histological type	977			
Infiltrating Ductal Carcinoma	772	Reference		
Infiltrating Lobular Carcinoma	205	0.827 (0.526-1.299)		0.41
PR status	1029			
Negative	342	Reference		
Positive	687	0.732 (0.523-1.024)		0.068
ER status	1032			
Negative	240	Reference		
Positive	792	0.712 (0.495-1.023)		0.066
HER2 status	715			
Negative	558	Reference		
Positive	157	1.593 (0.973-2.609)		0.064
Menopause status	931			
Pre	229	Reference		
Post	702	2.165 (1.302-3.600)		0.003
PIMREG	1082			
Low	541	Reference		
High	541	1.475 (1.070-2.034)		0.018

Figure 7 **Forest plot of univariate analysis of the correlation between clinicopathological characteristics and overall survival in BRCA.** Reference as the control group, blue dots as the estimated HR value, and black lines as 95% confidence interval of HR, sample size = 1109.
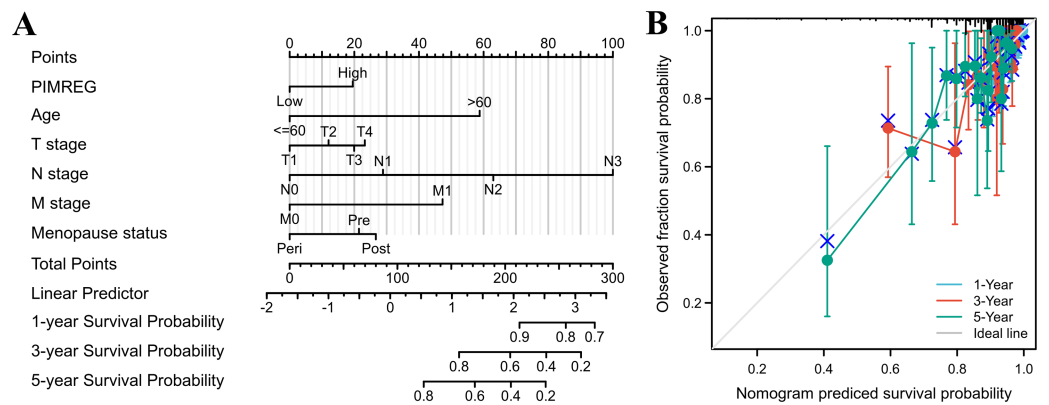
Full-size ⬒ DOI: 10.7717/peerj.15703/fig-7

Figure 8 **The predicting role of PIMREG regarding the prognosis of BRCA patients (sample size = 1109).** (A) Nomogram curve. The value of each variable was given a score on the point scale axis. The total score could be easily calculated by adding every score to predict the 1-, 3-, and 5-year survival probability (B) Calibration curve. The 45-degree line represents an ideal match between the actual survival (Y-axis) and nomogram-predicted survival (X-axis) and the perpendicular line means 95% confidence intervals.
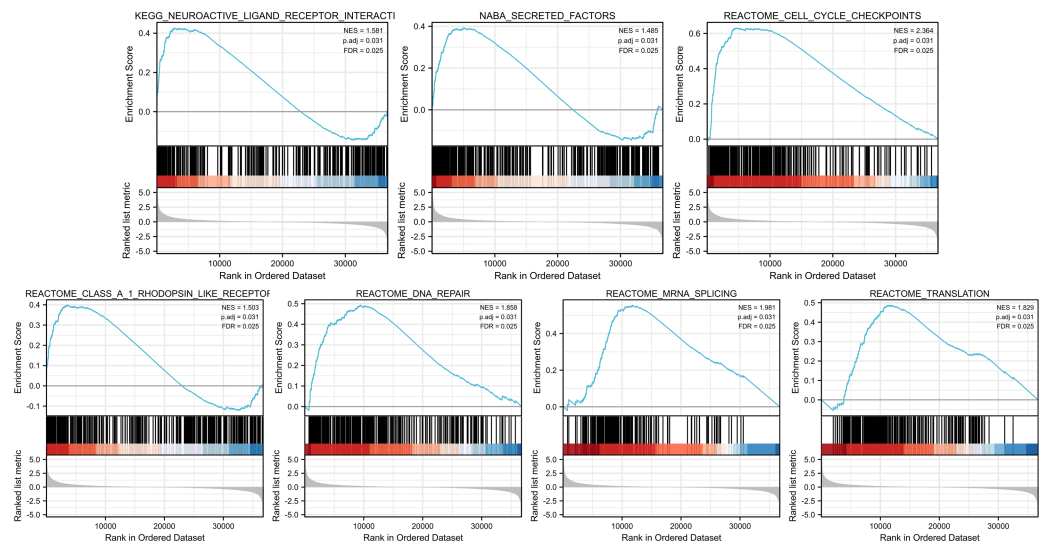
Full-size ⬒ DOI: 10.7717/peerj.15703/fig-8

Figure 9 GSEA web server results of the comparison between high PIMREG expression and low expression in breast cancer (sample size = 1109). NES: normalized enrichment score; p. adj; adjusted *p*-value; FDR: false discovery rate.

and human leukocyte antigen-A (HLA-A) showed significant associations with PIMREG (Figs. 11G–11I). These findings suggest that PIMREG may be involved in immune cell infiltration and immune modulation in breast cancer.

Relationship between PIMREG and immune checkpoints in BC

The relationship between PIMREG and immune checkpoints, including PD1 (PDCD1), PD1-L1 (CD274), and CTLA-4, which play a crucial role in tumor immune evasion, was assessed (*Zhang et al., 2021*). According to the analysis of TIMER data, PIMREG expression showed a relatively strong positive correlation with CTLA-4 only in BRCA (invasive breast carcinoma). This correlation was further adjusted by tumor purity using partial Spearman's correlation (Fig. 12A). However, the analysis using GEPIA data did not find a significant positive correlation between PIMREG and PD1 (PDCD1), PD1-L1 (CD274), and CTLA-4 (Figs. 12B–12D).These findings suggest that the relationship between PIMREG and immune checkpoints may vary depending on the specific analysis method and dataset used. Further studies are needed to explore the potential interactions between PIMREG and immune checkpoints in breast cancer.

Other genes/proteins interacted with PIMREG in patients with BC

GeneMANIA analysis revealed that PIMREG is implicated in various functions, including protein deacetylation, CHD-type complex, transcription repressor complex, histone deacetylase complex, ATPase complex, and SWI/SNF superfamily-type complex. The top 20 interactors associated with PIMREG included phosphatidylinositol binding clathrin assembly protein (PICALM), Tudor domain-containing 7 (TDRD7), RB binding protein 7 (RBBP7), RB binding protein 4 (RBBP4), metastasis-associated 1 family member 2 (MTA2), histone deacetylase 2 (HDAC2), suppressor APC domain-containing 2 (SAPCD2), kinesin
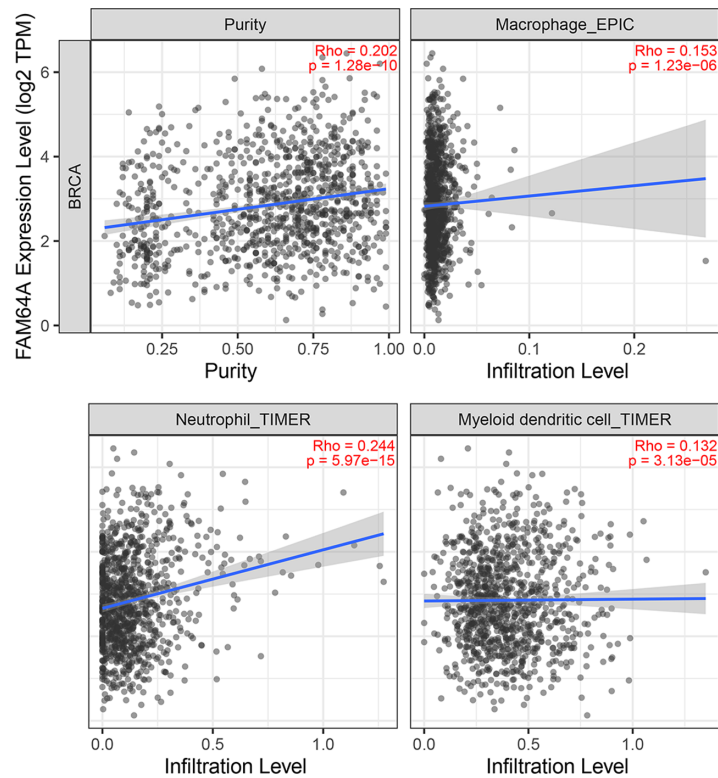
Figure 10 The association between levels of immune infiltrating cells and PIMREG expression in breast cancer. Sample size = 1109, dots represent gene expression , blue lines represent linear association and dark grey areas represent the 95% confidence intervals.

family member 15 (KIF15), chromatin licensing and DNA replication factor 1 (CDT1), histone deacetylase 1 (HDAC1), prion protein (PRNP), PHD finger protein 19 (PHF19), thymidylate synthetase (TYMS), zyg-11 family member B (ZYG11B), cyclin E1 (CCNE1), BUB1 mitotic checkpoint serine/threonine kinase (BUB1), ubiquitin-associated and SH3 domain-containing B (UBASH3B), SPC24 component of NDC80 kinetochore complex (SPC24), BLM RecQ like helicase (BLM), and transforming acidic coiled-coil-containing protein 3 (TACC3) (Fig. 13A).

Network analysis using MaxLink of BRCA1, BRCA2, and PIMREG revealed that MTA2, Cell Division Cycle 20 (CDC20), HDAC2, and Cyclin-Dependent Kinase 1 (CDK1) were important links connecting PIMREG with BRCA1/2 (Fig. 13B). Among these links, HDAC2 was the only direct connection between PIMREG and both BRCA1 and BRCA2, and MTA2 and HDAC2 were identified as interactors *via* GeneMANIA.

Investigate potential drugs that demonstrate interaction with PIMREG in BC

Using Q-omics (version 1.0), we analyzed 493 potential drugs. Among them, we identified 46 drugs that positively responded to increased expression of PIMREG (Fig. 14). The selection of these drugs was based on the Y-score, which represents the log (fold-change)
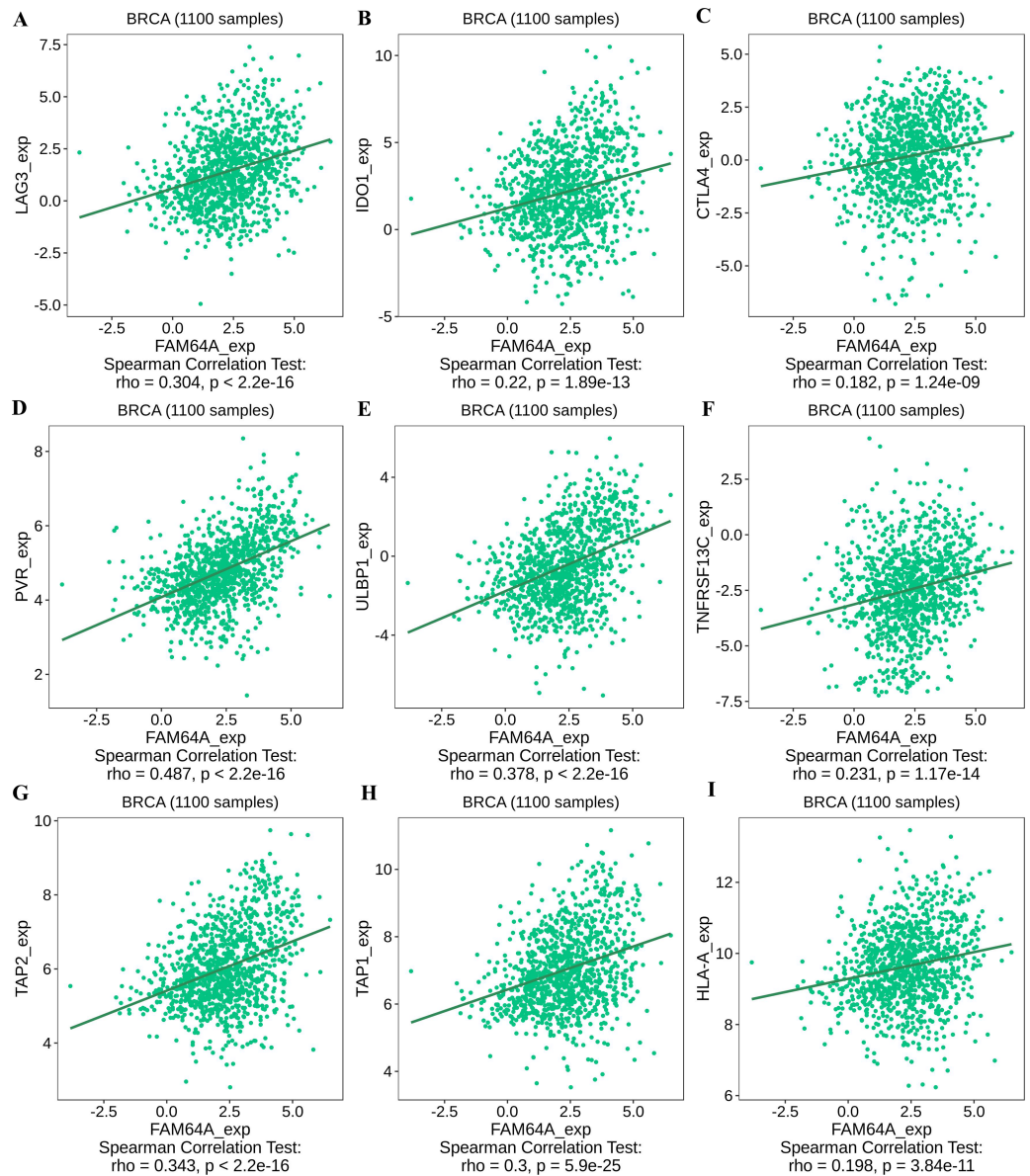
Figure 11 **The correlation between the PIMREG expression level and immunomodulators in breast cancer based on TISIDB (sample size = 1100,dots represent gene expression and lines represent linear association).** (A–C) Immunomodulators that are highly correlated with PIMEG; (D–F) immunomodulators that are highly correlated with PIMREG; (G–I) MHC molecules that are highly correlated with PIMREG.

Full-size ☒ DOI: 10.7717/peerj.15703/fig-11

of the drug response between samples with high PIMREG expression and samples with low PIMREG expression. The top three responsive drugs, based on the Y-score, were Mitoxantrone, Bleomycin, and AZD7762. For more detailed information about these potential drugs, please refer to Supplementary File 1.
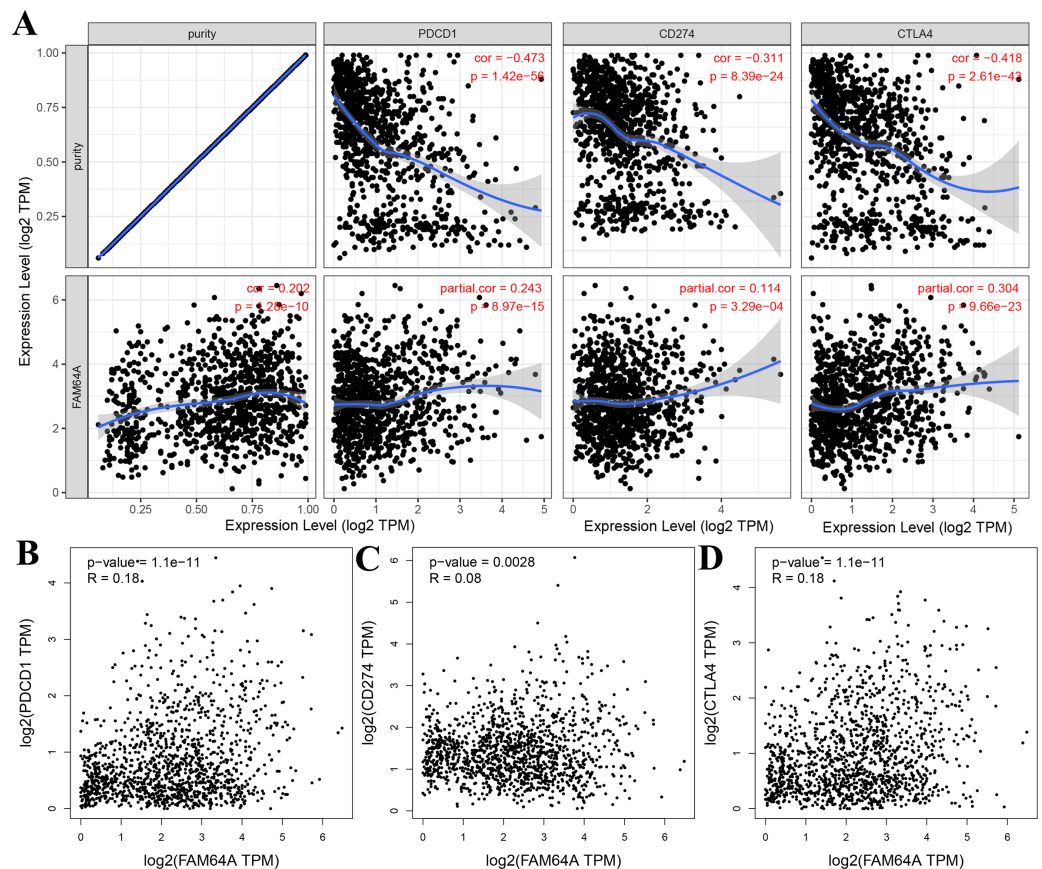
Figure 12 **Correlation of PIMREG expression with PDCD1, CD274, and CTLA-4 expression in breast cancer (sample size = 1109, dots represent gene expression , blue lines represent linear association and dark grey areas represent the 95% confidence intervals).** (A) Spearman correlation of PIMREG with expression of PDCD1, CD274, and CTLA-4 in breast cancer. (B) The expression correlation of PIMREG with PDCD1 in breast cancer. (C) The expression correlation of PIMREG with CD274 in breast cancer. (D) The expression correlation of PIMREG with CTLA-4 in breast cancer.

Full-size ⊡ DOI: 10.7717/peerj.15703/fig-12

Knockdown of PIMREG decreased the cell proliferation and migration in MDA-MB-231 cells

As anticipated, both qRT-PCR and western blot assays revealed the overexpression of PIMREG in BC cells when compared to normal human mammary epithelial cells (Figs. 15A–15B, $P < 0.01$). The western blot assay conducted on tissue samples (Fig. 15C, $P < 0.01$) and the experimental IHC assay (Fig. 15D) further confirmed the overexpression of PIMREG in BC tissue samples. To assess the impact of PIMREG on cell proliferation and migration, siRNA was employed to knockdown PIMREG expression (Figs. 15E–15F, $P < 0.01$). Following transfection with PIMREG-siRNA, both the CCK8 assay and transwell migration assay demonstrated a significant reduction in cell proliferation and migration in MDA-MB-231 cells when compared to the untreated group (Figs. 15G–15H, $P < 0.01$). These findings suggest that PIMREG may play a crucial role in BC cell proliferation and migration. Additionally, the colony formation assay was conducted to verify the effects
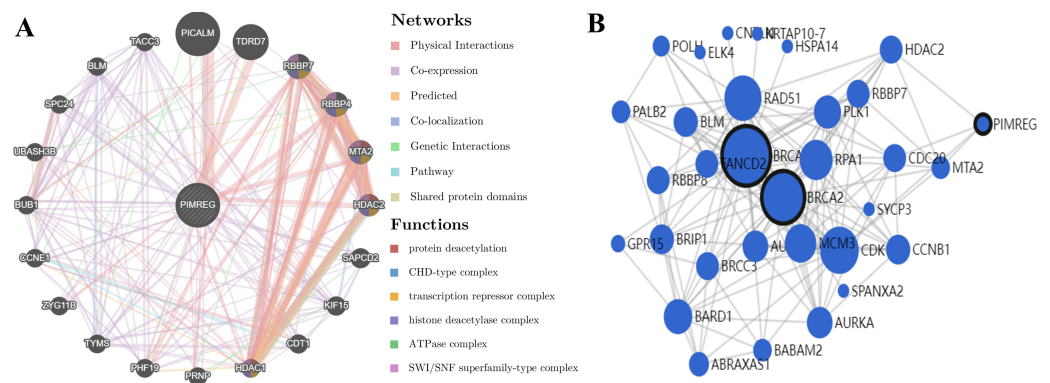
Figure 13   PPI interactions: (A) Interactions between other proteins and PIMREG in patients with breast cancer by GeneMANIA. (edge thickness represents interaction strength, color represents interaction type, node size represents protein score) (B) Network analysis of BRCA1, BRCA2, and PIMERG *via* MaxLink (node size represents the connectivity score).

Full-size 🖼 DOI: 10.7717/peerj.15703/fig-13
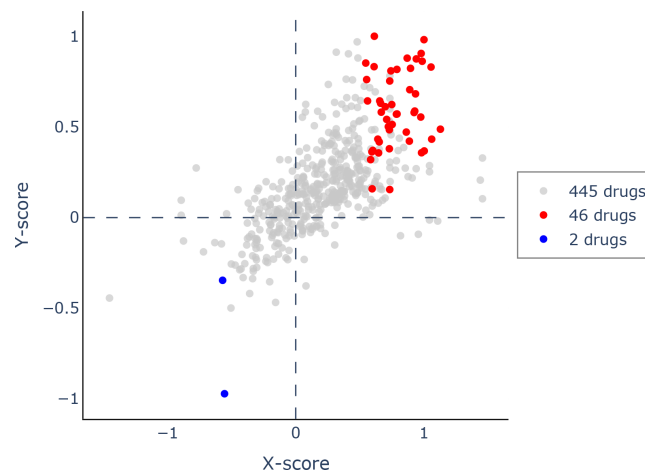
Figure 14   Scatter plot of drug response to PIMREG *via* Q-omics. Red dots and blue dots indicated the positive response and negative response, respectively.

Full-size 🖼 DOI: 10.7717/peerj.15703/fig-14

of HDAC2 (Fig. 15I). The results demonstrated that the colony formation ability of MDA-MB-231 cells was reduced after the knockdown of HDAC2, indicating that HDAC2 may serve as a potential therapeutic target for breast cancer.

DISCUSSION

BC is the most prevalent cancer type and a leading cause of tumor-associated mortality (15.5%) among females worldwide (*Sung et al., 2021*). Late-stage diagnosis, metastasis, and disease progression can result in irreversible consequences. However, timely detection and effective therapeutic interventions can significantly improve patient survival (*Barba et al., 2021*). Therefore, there is an urgent need to identify novel biomarkers that hold clinical and prognostic significance in BC. Additionally, the search for promising therapeutic targets
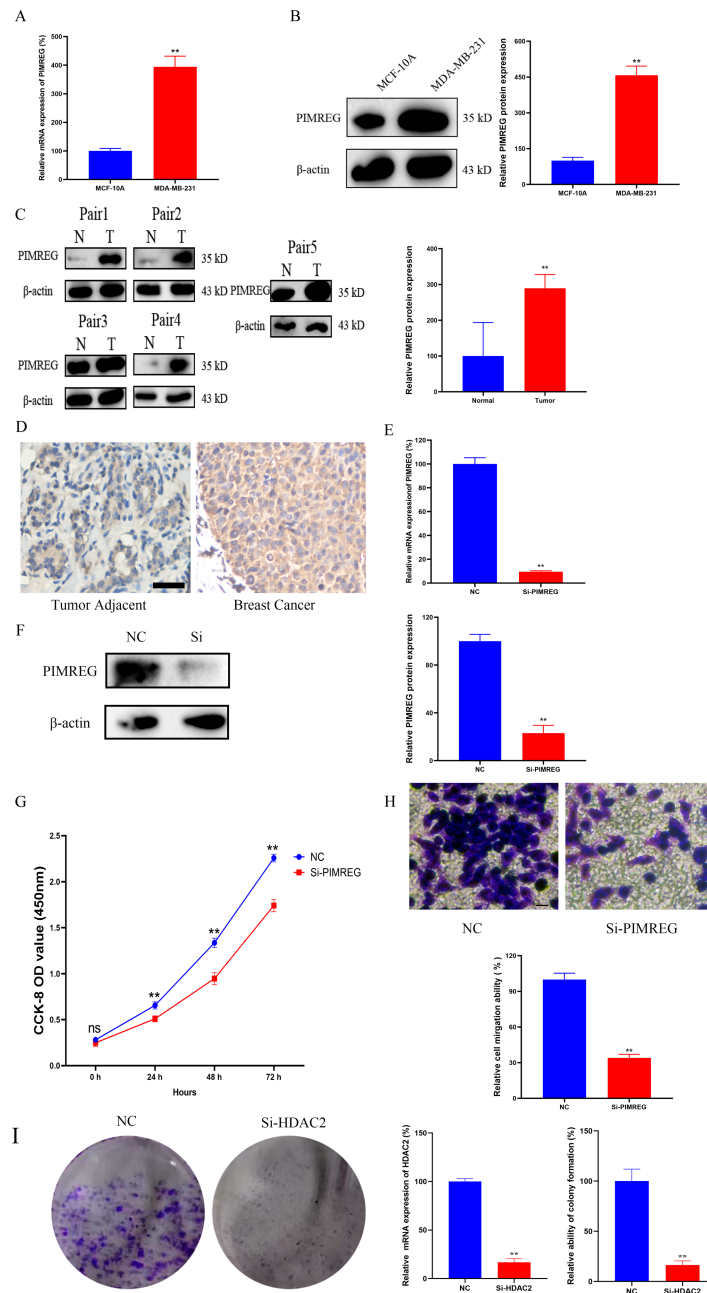
Figure 15 Effects of PIMREG on BC cell proliferation and migration. (A–B) mRNA and protein expression of PIMREG in MCF-10A and MDA-MB-231. (C) Protein expression of PIMREG in BC tissues and matched adjacent normal tissues. (D) IHC assay of PIMREG in BC tissues and matched adjacent normal tissues (Scar bar = 10 μm). (E–F) mRNA and protein expression of PIMREG in MDA-MB-231 cells transfected with siRNA- PIMREG. (G–H) cell proliferation and migration in MDA-MB-231 cells transfected with siRNA- PIMREG (Scar bar = 5 μm) colony formation ability in MDA-MB-231 cells transfected with siHDAC2. Data are presented as the mean ± standard deviation. ** $p < 0.01$ *versus* Normal group or NC group.

Full-size 🖼 DOI: 10.7717/peerj.15703/fig-15

for anti-tumor drug development is crucial in order to enhance overall survival and delay tumor progression.

In this study, we conducted an assessment of the expression pattern of PIMREG across different subtypes of BC. Our findings align with previous literature, highlighting the crucial role of PIMREG in promoting the formation of breast cancer cells (*Yamada et al., 2018*). According to our study, bioinformatic analysis and western blot analysis showed that PIMREG expression levels were significantly higher than in normal tissues, which is consistent with the findings of the previous study (*Yao et al., 2019*). Furthermore, PIMREG showed high expression in advanced pathologic stages of BC. Additionally, receptor profiling revealed lower expression of PIMREG in estrogen receptor-positive (ER+) and progesterone receptor-positive (PR+) BC cases (*Yao et al., 2019*). In situations where accurate classification or controversy arises regarding ER or PR status, PIMREG could serve as a useful distinguishing marker to aid physicians in diagnosis. Histologically, PIMREG exhibited more substantial upregulation in infiltrating ductal carcinoma than infiltrating lobular carcinoma. Thus, the localization of this gene could be utilized as a supplemental biomarker to assist in the differential diagnosis between these subtypes.

We conducted further exploration of the impact of PIMREG overexpression on the prognostic outcome of BC. Our findings, based on a larger cohort of patients with diverse backgrounds, are consistent with a previous study indicating that overall survival (OS), disease-specific survival (DSS), and progression-free interval (PFI) are negatively associated with high expression of PIMREG (*Jiang et al., 2019*). The AUC value further confirms its good prognostic value, and analysis of data from the GEO database confirms its negative association with OS. Moreover, our *in vitro* study demonstrated that the knockdown of PIMREG in MDA-MB-231 cells decreased cell proliferation and migration. The poor prognosis associated with PIMREG overexpression may be attributed to excessive NF-κB signaling, inhibition of the negative feedback loop, epithelial-to-mesenchymal transition (EMT), and enhanced breast cancer stemness (*Yao et al., 2019*; *Zhang et al., 2019*). Furthermore, PIMREG expression is negatively associated with survival in the infiltrating lobular carcinoma subtype. This pattern could potentially be explained by the influence of constitutive activation of AKT, which is a hallmark mutation of infiltrating lobular carcinoma. This activation amplifies downstream NF-κB signaling, ultimately promoting tumor cell survival and proliferation (*Pramod et al., 2021*). However, it is important to note that the survival analysis based on PAM50 subtypes did not reach statistical significance, limiting its use in prognostic prediction. The limited sample size in each subgroup could contribute to this lack of significance, and future studies with larger sample sizes are needed to clarify the clinical significance of PIMREG in different PAM50 subtypes of BC.

An extensive evaluation of PIMREG outcomes, combined with univariate analysis and other clinically relevant patterns, was performed to develop a nomogram. The calibration plot demonstrated favorable consistency between the actual and predicted values for 1-, 3-, and 5-year survival. To provide personalized scores for individual patients, the model incorporated complementary perspectives specific to their respective tumors.

Consequently, our nomogram has the potential to serve as an invaluable prognostic tool for physicians.

To explore the mechanism underlying the prognostic value of PIMREG, GSEA was conducted. The results revealed several pathways and processes potentially implicated in its prognostic significance, including neuroactive ligand receptor interaction, Naba secreted factors, cell cycle checkpoints, Class A/1 rhodopsin-like receptors, DNA repair, mRNA repair, and translation. Notably, the association between PIMREG and Naba secreted factors, previously identified by *Naba et al. (2016)* highlights their relevance to extracellular matrix (ECM) proteins. ECM is known to be a critical component of metastatic niches and plays a pivotal role in breast cancer metastasis (*Hebert et al., 2020*). Furthermore, the involvement of cell cycle checkpoints suggests a potential role in promoting cell cycle arrest in breast cancer cells (*Akbarzadeh et al., 2022*; *Cao et al., 2022*; *Markowicz-Piasecka et al., 2022*).

Tumor growth and metastasis are highly dependent on the complex tumor microenvironment (TME) and the extracellular matrix (ECM) (*Hanahan & Coussens, 2012*; *Oliver et al., 2018*). The ECM serves as a multifaceted network that not only provides structural support but also supplies biochemical factors and imparts biomechanical cues crucial for tumorigenesis (*Buoncervello, Gabriele & Toschi, 2019*). Furthermore, an analysis of the relationship between PIMREG and tumor-infiltrating immune cells in breast cancer revealed positive correlations with macrophages, neutrophils, and dendritic cells (DCs). Previous studies have linked macrophage infiltration to poor prognosis in breast cancer (*Mehta et al., 2021*). Recent advancements have also highlighted the key role of neutrophils in breast cancer progression and metastasis (*Yang et al., 2021*). Moreover, DCs have been extensively investigated as potential targets in cancer therapy, and studies have shown that combining autologous dendritic cells with activated cytotoxic T cells may represent a novel approach for breast cancer treatment (*Shevchenko et al., 2020*).

The investigation of therapies targeting immunomodulators has also shed light on immune infiltrating cells. In line with our study findings, which indicate higher expression of PIMREG in ER-negative and PR-negative groups, this provides additional evidence of a potential positive association between PIMREG expression and LAG3, a negative regulator of T cells. Another immunoinhibitory pathway of interest is IDO1, a rate-limiting oxidoreductase (*Macchiarulo et al., 2009*), which is currently being explored as part of combined photodynamic therapy and checkpoint blockade immunotherapy for triple-negative breast cancer (*Wu et al., 2021*). Although CTLA-4 ranked third in terms of correlation with PIMREG, it only demonstrated a trend towards conventional positive correlation levels, and further studies on therapies targeting CTLA-4 in breast cancer are still necessary. Our study also identified immunostimulatory agents, such as ULBP1, which activates NK cells and exerts tumor-killing effects (*Qi et al., 2021*; *Wang et al., 2020*), and TNFRSF13C, which promotes cancer cell death (*Abo-Elfadl et al., 2020*; *Bhat et al., 2013*; *Véquaud et al., 2015*). The transporter associated with antigen processing (TAP) plays a critical role in peptide delivery, and cancer cells can modulate TAP1 and/or TAP2 levels to reduce peptide delivery, thereby evading recognition by cytotoxic CD8+ T cells (*El Hage, Durgeau & Mami-Chouaib, 2013*). HLA-A, a well-known major histocompatibility complex

(MHC) molecule, has been linked to prognosis in basal-like and HER2-enriched breast cancer subtypes (*Noblejas-López et al., 2019*).

In our study, we also investigated immune checkpoints, specifically PD-1, PD-L1, and CTLA-4, which are known to negatively regulate T-cell immune response. Activation of PD-1 by PD-L1 leads to a reduction in T-cell activity, cytokine production, and tolerance to antigens. Pembrolizumab, a PD-L1 inhibitor, has been tested in early phase clinical trials for metastatic PD-L1-positive triple-negative breast cancer (TNBC) and has shown clinical benefits in approximately 20% of patients (*Nanda et al., 2016*). However, our study did not reveal a significant correlation between PIMREG and PD-1/PD-L1, suggesting that PIMREG expression may not be a reliable biomarker for predicting the response to immunotherapies targeting PD-1/PD-L1. As for CTLA-4, previous studies have indicated that combining anti-CTLA-4 with anti-PD-1/PD-L1 may be a viable second-line therapy for BC (*Kern & Panis, 2021*; *Sun et al., 2020*). Our findings, based on TIMER analysis, suggested a correlation between PIMREG and CTLA-4, but further studies are needed to validate this correlation.

Apart from potential immunotherapies, exploration of other potential drugs that positively respond to PIMREG in BC was performed by using Via Q-omics. Mitoxantrone, a synthetic anthracycline anticancer drug, can produces antitumor effects by the inhibition of Toll-like receptor 4 (TLR4) and NF-κB activation (*Evison et al., 2016*; *Rinne et al., 2020*). Mitoxantrone-based chemotherapy used to be a chemotherapeutic drug for BC decades ago (*Hainsworth et al., 1991*). Bleomycin is a commonly used medication for various malignancies, and it has recently gained favor as part of electrochemotherapy for cutaneous and subcutaneous metastases of BC (*Esposito et al., 2021*; *Ferioli et al., 2021*; *Russano et al., 2021*). AZD7762 is a selective checkpoint kinases 1 and 2 inhibitor, and a previous meta-analysis suggested an association between checkpoint kinase 2 mutation and increased risk of BC (*Liang et al., 2018*; *Ma et al., 2012*; *Park et al., 2016*). Therefore, AZD7762 is a promising drug in BC treatment which requires more evaluation.

To explore additional potential therapeutic targets, we investigated the relationship between PIMREG and BRCA1/2, as well as proteins highly associated with PIMREG. Although the specific mechanism and pathway interactions through which PIMREG promotes breast cancer remain unknown (*Archangelo et al., 2008*), our study identified correlations between PIMREG and MTA2, and HDAC2. MTA2 is known to deacetylate ER alpha and p53, inhibiting their transactivation function and potentially affecting breast cancer progression (*Cui et al., 2006*). HDAC2, a member of the histone deacetylase family, is located in the nucleus, and its overexpression has been associated with lymph node invasion, higher grade, and poor prognosis in breast cancer (*Darvishi et al., 2020*). Interestingly, our study revealed that HDAC2 is the only direct link between PIMREG and BRCA1 and BRCA2. BRCA1 and BRCA2 are well-known genetic factors involved in DNA repair and are associated with a strong predisposition for early-onset familial breast cancer (*Toh et al., 2008*). Furthermore, our colony formation assay results indicated that HDAC2 may serve as a potential therapeutic target for breast cancer. Based on the findings of our study and previous research, MTA2 and HDAC2 show promise as potential targets for breast cancer treatment.

However, this study has several limitations that should be considered. First, the datasets used for bioinformatic analysis were obtained from different databases and platforms, which may introduce uncertain systematic bias and potentially lead to misinterpretation of the data. Second, the enrichment analysis conducted to assess the regulatory function of PIMREG was preliminary and further experimental validation is necessary. Third, additional investigations are required to explore the interaction of potential drugs with PIMREG and their effects on breast cancer patients with high PIMREG expression. Fourth, the underlying mechanism of PIMREG in breast cancer remains largely unknown, and further *in vitro* and *in vivo* studies are needed to gain a deeper understanding.

CONCLUSION

In summary, PIMREG is upregulated in BC tissues, and its high expression correlates with poor BC prognosis and immune infiltrates in BC. Among the proteins associated with PIMREG, HDAC2 might serve as a critical link between PIMREG and BRCA1/2, and thus could be a potential therapeutic target for future research. Potential immunomodulators, and immune checkpoints correlated with PIMREG were also identified in this study, indicating potential values of immunomodulatory drugs and immune checkpoint inhibitors in BC. Mitoxantrone, Bleomycin, and AZD7762 may respond well to PIMREG. Therefore, future studies are needed to further explore their therapeutic values.

ACKNOWLEDGEMENTS

ADDITIONAL INFORMATION AND DECLARATIONS

Competing Interests

The authors declare there are no competing interests.

Author Contributions

- Wenjing Zhao performed the experiments, authored or reviewed drafts of the article, and approved the final draft.
- Yuanjin Chang performed the experiments, authored or reviewed drafts of the article, and approved the final draft.
- Zhaoye Wu performed the experiments, analyzed the data, authored or reviewed drafts of the article, and approved the final draft.
- Xiaofan Jiang performed the experiments, authored or reviewed drafts of the article, and approved the final draft.
- Yong Li performed the experiments, authored or reviewed drafts of the article, and approved the final draft.
- Ruijin Xie performed the experiments, analyzed the data, prepared figures and/or tables, authored or reviewed drafts of the article, and approved the final draft.
- Deyuan Fu analyzed the data, prepared figures and/or tables, and approved the final draft.
- Chenyu Sun conceived and designed the experiments, prepared figures and/or tables, and approved the final draft.
- Ju Gao conceived and designed the experiments, authored or reviewed drafts of the article, and approved the final draft.

Human Ethics

The following information was supplied relating to ethical approvals (i.e., approving body and any reference numbers):

All the patients involved in this study signed a written informed consent and this study was approved by the ethics committee of Northern Jiangsu People's Hospital Affiliated to Yangzhou University (Approval ID: 2022KY316).

Data Availability

The following information was supplied regarding data availability:

The raw data, including original Western blots, are available in the Supplemental Files.

Supplemental Information

Supplemental information for this article can be found online at http://dx.doi.org/10.7717/peerj.15703#supplemental-information.

REFERENCES

Abo-Elfadl MT, Gamal-Eldeen AM, Ismail MF, Shahin NN. 2020. Silencing of the cytokine receptor TNFRSF13B: a new therapeutic target for triple-negative breast cancer. *Cytokine* **125**:154790 DOI 10.1016/j.cyto.2019.154790.

Akbarzadeh I, Farid M, Javidfar M, Zabet N, Shokoohian B, Arki MK, Shpichka A, Noorbazargan H, Aghdaei HA, Hossein-Khannazer N, Timashev P, Makvandi P, Vosough M. 2022. The optimized formulation of tamoxifen-loaded niosomes efficiently induced apoptosis and cell cycle arrest in breast cancer cells. *AAPS PharmSciTech* **23**:57 DOI 10.1208/s12249-022-02212-0.

Archangelo LF, Greif PA, Hölzel M, Harasim T, Kremmer E, Przemeck GK, Eick D, Deshpande AJ, Buske C, De Angelis MH, Saad ST, Bohlander SK. 2008. The CALM and CALM/AF10 interactor CATS is a marker for proliferation. *Molecular Oncology* **2**:356–367 DOI 10.1016/j.molonc.2008.08.001.

Arnedos M, Roulleaux Dugage M, Perez-Garcia J, Cortes J. 2019. Window of opportunity trials for biomarker discovery in breast cancer. *Current Opinion in Oncology* **31**:486–492 DOI 10.1097/cco.0000000000000583.

Balachandran VP, Gonen M, Smith JJ, De Matteo RP. 2015. Nomograms in oncology: more than meets the eye. *The Lancet Oncology* **16**:e173–e180 DOI 10.1016/s1470-2045(14)71116-7.

Barba D, León-Sosa A, Lugo P, Suquillo D, Torres F, Surre F, Trojman L, Caicedo A. 2021. Breast cancer, screening and diagnostic tools: all you need to know. *Critical Reviews in Oncology/Hematology* **157**:103174 DOI 10.1016/j.critrevonc.2020.103174.

Barbutti I, Xavier-Ferrucio JM, Machado-Neto JA, Ricon L, Traina F, Bohlander SK, Saad ST, Archangelo LF. 2016. CATS (FAM64A) abnormal expression reduces clonogenicity of hematopoietic cells. *Oncotarget* **7**:68385–68396 DOI 10.18632/oncotarget.11724.

Bhat KPL, Balasubramaniyan V, Vaillant B, Ezhilarasan R, Hummelink K, Hollingsworth F, Wani K, Heathcock L, James JD, Goodman LD, Conroy S, Long L, Lelic N, Wang S, Gumin J, Raj D, Kodama Y, Raghunathan A, Olar A, Joshi K, Pelloski CE, Heimberger A, Kim SH, Cahill DP, Rao G, Den Dunnen WFA, Boddeke H, Phillips HS, Nakano I, Lang FF, Colman H, Sulman EP, Aldape K. 2013. Mesenchymal differentiation mediated by NF-κB promotes radiation resistance in glioblastoma. *Cancer Cell* **24**:331–346 DOI 10.1016/j.ccr.2013.08.001.

Breastcancer.org. 2023. Breast cancer facts & stats. *Available at* https://www.breastcancer.org/facts-statistics (accessed on 06 August 2023).

Buoncervello M, Gabriele L, Toschi E. 2019. The Janus face of tumor microenvironment targeted by immunotherapy. *International Journal of Molecular Sciences* **20(17)**:4320 DOI 10.3390/ijms20174320.

Cao W, Shen R, Richard S, Liu Y, Jalalirad M, Cleary MP, D'Assoro AB, Gradilone SA, Yang DQ. 2022. Inhibition of triple-negative breast cancer proliferation and motility by reactivating p53 and inhibiting overactivated Akt. *Oncology Reports* **47**:41 DOI 10.3892/or.2021.8252.

Clarke C, Madden SF, Doolan P, Aherne ST, Joyce H, O'Driscoll L, Gallagher WM, Hennessy BT, Moriarty M, Crown J, Kennedy S, Clynes M. 2013. Correlating transcriptional networks to breast cancer survival: a large-scale coexpression analysis. *Carcinogenesis* **34**:2300–2308 DOI 10.1093/carcin/bgt208.

Cui Y, Niu A, Pestell R, Kumar R, Curran EM, Liu Y, Fuqua SA. 2006. Metastasis-associated protein 2 is a repressor of estrogen receptor alpha whose overexpression leads to estrogen-independent growth of human breast cancer cells. *Molecular Endocrinology* **20**:2020–2035 DOI 10.1210/me.2005-0063.

Darvishi N, Rahimi K, Mansouri K, Fathi F, Menbari MN, Mohammadi G, Abdi M. 2020. MiR-646 prevents proliferation and progression of human breast cancer cell lines by suppressing HDAC2 expression. *Molecular and Cellular Probes* **53**:101649 DOI 10.1016/j.mcp.2020.101649.

De Velasco G, Je Y, Bossé D, Awad MM, Ott PA, Moreira RB, Schutz F, Bell-munt J, Sonpavde GP, Hodi FS, Choueiri TK. 2017. Comprehensive meta-analysis of key immune-related adverse events from CTLA-4 and PD-1/PD-L1 inhibitors in cancer patients. *Cancer Immunology Research* **5**:312–318 DOI 10.1158/2326-6066.Cir-16-0237.

Ding Y, Liu N, Chen M, Xu Y, Fang S, Xiang W, Hua X, Chen G, Zhong Y, Yu H. 2021. Overexpressed pseudogene MT1L associated with tumor immune infiltrates and indicates a worse prognosis in BLCA. *World Journal of Surgical Oncology* **19**:133 DOI 10.1186/s12957-021-02231-4.

Ding J, Zhao S, Chen X, Luo C, Peng J, Zhu J, Shen Y, Luo Z, Chen J. 2022. Prognostic and diagnostic values of Semaphorin 5B and its correlation with tumor-infiltrating immune cells in kidney renal clear-cell carcinoma. *Frontiers in Genetics* **13**:835355 DOI 10.3389/fgene.2022.835355.

Duffy MJ, Walsh S, McDermott EW, Crown J. 2015. Biomarkers in breast cancer: where are we and where are we going? *Advances in Clinical Chemistry* **71**:1–23 DOI 10.1016/bs.acc.2015.05.001.

El Hage F, Durgeau A, Mami-Chouaib F. 2013. TAP expression level in tumor cells defines the nature and processing of MHC class I peptides for recognition by tumor-specific cytotoxic T lymphocytes. *Annals of the New York Academy of Sciences* **1283**:75–80 DOI 10.1111/j.1749-6632.2012.06777.x.

Esposito E, Siani C, Pace U, Costanzo R, Di Giacomo R. 2021. Debulking mastectomy with electrochemotherapy: a case report of no surgery approach to recurrent breast cancer. *Translational Cancer Research* **10**:1144–1149 DOI 10.21037/tcr-20-2803.

Evison BJ, Sleebs BE, Watson KG, Phillips DR, Cutts SM. 2016. Mitoxantrone, more than just another topoisomerase II poison. *Medicinal Research Reviews* **36**:248–299 DOI 10.1002/med.21364.

Ferioli M, Perrone AM, Buwenge M, Arcelli A, Zamagni A, Macchia G, Deodato F, Cilla S, Tagliaferri L, De Terlizzi F, De Iaco P, Zamagni C, Morganti AG. 2021. Electrochemotherapy of skin metastases from breast cancer: a systematic review. *Clinical and Experimental Metastasis* **38**:1–10 DOI 10.1007/s10585-020-10063-x.

Grenier JM, Yeung ST, Khanna KM. 2018. Combination immunotherapy: taking cancer vaccines to the next level. *Frontiers in Immunology* **9**:610 DOI 10.3389/fimmu.2018.00610.

Guala D, Sjölund E, Sonnhammer EL. 2014. MaxLink: network-based prioritization of genes tightly linked to a disease seed set. *Bioinformatics* **30**:2689–2690 DOI 10.1093/bioinformatics/btu344.

Hainsworth JD, Andrews MB, Johnson DH, Greco FA. 1991. Mitoxantrone, fluorouracil, and high-dose leucovorin: an effective, well-tolerated regimen for metastatic breast cancer. *Journal of Clinical Oncology* **9**:1731–1735 DOI 10.1200/jco.1991.9.10.1731.

Hamann M, Grill S, Struck J, Bergmann A, Hartmann O, Pölcher M, Kiechle M. 2019. Detection of early breast cancer beyond mammographic screening: a promising biomarker panel. *Biomarkers in Medicine* **13**:1107–1117 DOI 10.2217/bmm-2019-0085.

Hanahan D, Coussens LM. 2012. Accessories to the crime: functions of cells recruited to the tumor microenvironment. *Cancer Cell* **21**:309–322 DOI 10.1016/j.ccr.2012.02.022.

He M, Han Y, Cai C, Liu P, Chen Y, Shen H, Xu X, Zeng S. 2021. CLEC10A is a prognostic biomarker and correlated with clinical pathologic features and immune infiltrates in lung adenocarcinoma. *Journal of Cellular and Molecular Medicine* **25**:3391–3399 DOI 10.1111/jcmm.16416.

Hebert JD, Myers SA, Naba A, Abbruzzese G, Lamar JM, Carr SA, Hynes RO. 2020. Proteomic profiling of the ECM of Xenograft breast cancer metastases in different organs reveals distinct metastatic niches. *Cancer Research* **80**:1475–1485 DOI 10.1158/0008-5472.Can-19-2961.

Iasonos A, Schrag D, Raj GV, Panageas KS. 2008. How to build and interpret a nomogram for cancer prognosis. *Journal of Clinical Oncology* **26**:1364–1370 DOI 10.1200/jco.2007.12.9791.

Jeong E, Lee Y, Kim Y, Lee J, Yoon S. 2020. Analysis of cross-association between mRNA expression and RNAi efficacy for predictive target discovery in colon cancers. *Cancers* **12(11)**:3091 DOI 10.3390/cancers12113091.

Jiang F, Liang M, Huang X, Shi W, Wang Y. 2021. High expression of PIMREG predicts poor survival outcomes and is correlated with immune infiltrates in lung adenocarcinoma. *PeerJ* **9**:e11697 DOI 10.7717/peerj.11697.

Jiang L, Ren L, Zhang X, Chen H, Chen X, Lin C, Wang L, Hou N, Pan J, Zhou Z, Huang H, Huang D, Yang J, Liang Y, Li J. 2019. Overexpression of PIMREG promotes breast cancer aggressiveness via constitutive activation of NF-κB signaling. *EBioMedicine* **43**:188–200 DOI 10.1016/j.ebiom.2019.04.001.

Jin Y, Tan Y, Chen L, Liu Y, Ren Z. 2018. Reactive oxygen species induces lipid droplet accumulation in HepG2 cells by increasing perilipin 2 expression. *International Journal of Molecular Sciences* **19(11)**:3445 DOI 10.3390/ijms19113445.

Kern R, Panis C. 2021. CTLA-4 expression and its clinical significance in breast cancer. *Archivum Immunologiae et Therapiae Experimentalis (Warsz)* **69**:16 DOI 10.1007/s00005-021-00618-5.

Kim A, Ma JY. 2018. Rhaponticin decreases the metastatic and angiogenic abilities of cancer cells via suppression of the HIF-1α pathway. *International Journal of Oncology* **53**:1160–1170 DOI 10.3892/ijo.2018.4479.

Lee J, Kim Y, Jin S, Yoo H, Jeong S, Jeong E, Yoon S. 2021. Q-omics: smart software for assisting oncology and cancer research. *Molecular Cell* **44**:843–850 DOI 10.14348/molcells.2021.0169.

Li B, Severson E, Pignon JC, Zhao H, Li T, Novak J, Jiang P, Shen H, Aster JC, Rodig S, Signoretti S, Liu JS, Liu XS. 2016. Comprehensive analyses of tumor immunity: implications for cancer immunotherapy. *Genome Biology* **17**:174 DOI 10.1186/s13059-016-1028-7.

Li T, Fan J, Wang B, Traugh N, Chen Q, Liu JS, Li B, Liu XS. 2017. TIMER: a web server for comprehensive analysis of tumor-infiltrating immune cells. *Cancer Research* **77**:e108–e110 DOI 10.1158/0008-5472.Can-17-0307.

Liang M, Zhang Y, Sun C, Rizeq FK, Min M, Shi T, Sun Y. 2018. Association between CHEK2*1100delC and breast cancer: a systematic review and meta-analysis. *Molecular Diagnosis & Therapy* **22**:397–407 DOI 10.1007/s40291-018-0344-x.

Liu J, Lichtenberg T, Hoadley KA, Poisson LM, Lazar AJ, Cherniack AD, Kovatich AJ, Benz CC, Levine DA, Lee AV, Omberg L, Wolf DM, Shriver CD, Thorsson V, Hu H. 2018. An integrated TCGA pan-cancer clinical data resource to drive high-quality survival outcome analytics. *Cell* **173**:400–416 DOI 10.1016/j.cell.2018.02.052.

Liu S, Geng R, Lin E, Zhao P, Chen Y. 2021. ERBB1/2/3 expression, prognosis, and immune infiltration in cutaneous melanoma. *Frontiers in Genetics* **12**:602160 DOI 10.3389/fgene.2021.602160.

Lou W, Wang W, Chen J, Wang S, Huang Y. 2021. ncRNAs-mediated high expression of SEMA3F correlates with poor prognosis and tumor immune infiltration of hepatocellular carcinoma. *Molecular Therapy—Nucleic Acids* **24**:845–855 DOI 10.1016/j.omtn.2021.03.014.

Ma Z, Yao G, Zhou B, Fan Y, Gao S, Feng X. 2012. The Chk1 inhibitor AZD7762 sensitises p53 mutant breast cancer cells to radiation in vitro and in vivo. *Molecular Medicine Reports* **6**:897–903 DOI 10.3892/mmr.2012.999.

Macchiarulo A, Camaioni E, Nuti R, Pellicciari R. 2009. Highlights at the gate of tryptophan catabolism: a review on the mechanisms of activation and regulation of indoleamine 2, 3-dioxygenase (IDO), a novel target in cancer disease. *Amino Acids* **37**:219–229 DOI 10.1007/s00726-008-0137-3.

Markowicz-Piasecka M, Huttunen J, Zajda A, Sikora J, Huttunen KM. 2022. Sulfonamide metformin derivatives induce mitochondrial-associated apoptosis and cell cycle arrest in breast cancer cells. *Chemico-Biological Interactions* **352**:109795 DOI 10.1016/j.cbi.2021.109795.

Mayor S. 2015. Screening for early breast cancer reduces invasive cancer, study finds. *Bmj* **351**:h6576 DOI 10.1136/bmj.h6576.

Mehta AK, Kadel S, Townsend MG, Oliwa M, Guerriero JL. 2021. Macrophage biology and mechanisms of immune suppression in breast cancer. *Frontiers in Immunology* **12**:643771 DOI 10.3389/fimmu.2021.643771.

Naba A, Clauser KR, Ding H, Whittaker CA, Carr SA, Hynes RO. 2016. The extra-cellular matrix: tools and insights for the omics era. *Matrix Biology* **49**:10–24 DOI 10.1016/j.matbio.2015.06.003.

Najafi S, Sadeghi M, Abasvandi F, Shajari MR, Mohebi K, Ghandchi H. 2019. Prognostic factors influencing prognosis in early breast cancer patients. *Prz Menopauzalny* **18**:82–88 DOI 10.5114/pm.2019.86833.

Nanda R, Chow LQ, Dees EC, Berger R, Gupta S, Geva R, Pusztai L, Pathiraja K, Aktan G, Cheng JD, Karantza V, Buisseret L. 2016. Pembrolizumab in patients with advanced triple-negative breast cancer: phase Ib KEYNOTE-012 study. *Journal of Clinical Oncology* **34**:2460–2467 DOI 10.1200/jco.2015.64.8931.

Noblejas-López MDM, Nieto-Jiménez C, Morcillo García S, Pérez-Peña J, Nuncia-Cantarero M, Andrés-Pretel F, Galán-Moya EM, Amir E, Pandiella A, Győrffy B, Ocana A. 2019. Expression of MHC class I, HLA-A and HLA-B identifies immune-activated breast tumors with favorable outcome. *Oncoimmunology* **8**:e1629780 DOI 10.1080/2162402x.2019.1629780.

Oliver AJ, Lau PKH, Unsworth AS, Loi S, Darcy PK, Kershaw MH, Slaney CY. 2018. Tissue-dependent tumor microenvironments and their impact on immunotherapy responses. *Frontiers in Immunology* **9**:70 DOI 10.3389/fimmu.2018.00070.

Park JS, Lee C, Kim HK, Kim D, Son JB, Ko E, Cho JH, Kim ND, Nan HY, Kim CY, Yoon S, Lee SH, Choi HG. 2016. Suppression of the metastatic spread of breast cancer by DN10764 (AZD7762)-mediated inhibition of AXL signaling. *Oncotarget* **7**:83308–83318 DOI 10.18632/oncotarget.13088.

Pontén F, Schwenk JM, Asplund A, Edqvist PH. 2011. The human protein atlas as a proteomic resource for biomarker discovery. *Journal of Internal Medicine* **270**:428–446 DOI 10.1111/j.1365-2796.2011.02427.x.

Pramod N, Nigam A, Basree M, Mawalkar R, Mehra S, Shinde N, Tozbikian G, Williams N, Majumder S, Ramaswamy B. 2021. Comprehensive review of molecular mechanisms and clinical features of invasive lobular cancer. *Oncologist* **26**:e943–e953 DOI 10.1002/onco.13734.

Qi F, Du X, Zhao Z, Zhang D, Huang M, Bai Y, Yang B, Qin W, Xia J. 2021. Tumor mutation burden-associated LINC00638/miR-4732-3p/ULBP1 axis promotes immune escape via PD-L1 in hepatocellular carcinoma. *Frontiers in Oncology* **11**:729340 DOI 10.3389/fonc.2021.729340.

R Core Team. 2020. R: a language and environment for statistical computing. Version 3.6.3. Vienna: R Foundation for Statistical Computing. *Available at* https://www.r-project.org.

Rao X, Huang X, Zhou Z, Lin X. 2013. An improvement of the 2ˆ(-delta delta CT) method for quantitative real-time polymerase chain reaction data analysis. *Biostat Bioinforma Biomath* **3**:71–85.

Rinne M, Mätlik K, Ahonen T, Vedovi F, Zappia G, Moreira VM, Yli-Kauhaluoma J, Leino S, Salminen O, Kalso E, Airavaara M, Xhaard H. 2020. Mitoxantrone, pixantrone and mitoxantrone (2-hydroxyethyl)piperazine are toll-like receptor 4 antagonists, inhibit NF-κB activation, and decrease TNF-alpha secretion in

primary microglia. *European Journal of Pharmaceutical Science* **154**:105493 DOI 10.1016/j.ejps.2020.105493.

Russano F, Del Fiore P, Di Prata C, Pasqual A, Marconato R, Campana LG, Spina R, Gianesini CM, Collodetto A, Tropea S, Dall'Olmo L, Carraro S, Parisi A, Galuppo S, Scarzello G, De Terlizzi F, Rastrelli M, Mocellin S. 2021. The role of electrochemotherapy in the cutaneous and subcutaneous metastases from breast cancer: analysis of predictive factors to treatment from an Italian cohort of patients. *Frontiers in Oncology* **11**:772144 DOI 10.3389/fonc.2021.772144.

Shevchenko JA, Khristin AA, Kurilin VV, Kuznetsova MS, Blinova DD, Starostina NM, Sidorov SV, Sennikov SV. 2020. Autologous dendritic cells and activated cytotoxic T-cells as combination therapy for breast cancer. *Oncology Reports* **43**:671–680 DOI 10.3892/or.2019.7435.

Subramanian A, Tamayo P, Mootha VK, Mukherjee S, Ebert BL, Gillette MA, Paulovich A, Pomeroy SL, Golub TR, Lander ES, Mesirov JP. 2005. Gene set enrichment analysis: a knowledge-based approach for interpreting genome-wide expression profiles. *Proceedings of the National Academy of Sciences of the United States of America* **102**:15545–15550 DOI 10.1073/pnas.0506580102.

Sun T, Zhang W, Li Y, Jin Z, Du Y, Tian J, Xue H. 2020. Combination immunotherapy with cytotoxic T-lymphocyte-associated antigen-4 and programmed death protein-1 inhibitors prevents postoperative breast tumor recurrence and metastasis. *Molecular Cancer Therapeutics* **19**:802–811 DOI 10.1158/1535-7163.Mct-19-0495.

Sung H, Ferlay J, Siegel RL, Laversanne M, Soerjomataram I, Jemal A, Bray F. 2021. Global cancer statistics 2020: GLOBOCAN estimates of incidence and mortality worldwide for 36 cancers in 185 countries. *CA: A Cancer Journal for Clinicians* **71**:209–249 DOI 10.3322/caac.21660.

Toh GT, Kang P, Lee SS, Lee DS, Lee SY, Selamat S, Mohd Taib NA, Yoon SY, Yip CH, Teo SH. 2008. BRCA1 and BRCA2 germline mutations in Malaysian women with early-onset breast cancer without a family history. *PLOS ONE* **3**:e2024 DOI 10.1371/journal.pone.0002024.

Véquaud E, Séveno C, Loussouarn D, Engelhart L, Campone M, Juin P, Barillé-Nion S. 2015. YM155 potently triggers cell death in breast cancer cells through an autophagy-NF-kB network. *Oncotarget* **6**:13476–13486 DOI 10.18632/oncotarget.3638.

Vlasblom J, Zuberi K, Rodriguez H, Arnold R, Gagarinova A, Deineko V, Kumar A, Leung E, Rizzolo K, Samanfar B, Chang L, Phanse S, Golshani A, Greenblatt JF, Houry WA, Emili A, Morris Q, Bader G, Babu M. 2015. Novel function discovery with GeneMANIA: a new integrated resource for gene function prediction in Escherichia coli. *Bioinformatics* **31**:306–310 DOI 10.1093/bioinformatics/btu671.

Wang Y, Zhang H, Jiao B, Nie J, Li X, Wang W, Wang H. 2020. The roles of alternative splicing in tumor-immune cell interactions. *Current Cancer Drug Targets* **20**:729–740 DOI 10.2174/1568009620666200619123725.

Wu C, Xu J, Xie Z, Huang H, Li N, Wei X, Li T, Yang H, Li S, Qin X, Liu Y. 2021. Light-responsive hyaluronic acid nanomicelles co-loaded with an IDO inhibitor focus

targeted photoimmunotherapy against immune cold cancer. *Biomaterials Science* **9**:8019–8031 DOI 10.1039/d1bm01409a.

Xie R, Zhao W, Lowe S, Bentley R, Hu G, Mei H, Jiang X, Sun C, Wu Y, Yueying L. 2022. Quercetin alleviates kainic acid-induced seizure by inhibiting the Nrf2-mediated ferroptosis pathway. *Free Radical Biology and Medicine* **191**:212–226 DOI 10.1016/j.freeradbiomed.2022.09.001.

Xu F, Jin T, Zhu Y, Dai C. 2018. Immune checkpoint therapy in liver cancer. *Journal of Experimental & Clinical Cancer Research* **37**:110 DOI 10.1186/s13046-018-0777-4.

Xu H, Zou R, Li F, Liu J, Luan N, Wang S, Zhu L. 2021. MRPL15 is a novel prognostic biomarker and therapeutic target for epithelial ovarian cancer. *Cancer Medicine* **10**:3655–3673 DOI 10.1002/cam4.3907.

Yamada Y, Arai T, Kojima S, Sugawara S, Kato M, Okato A, Yamazaki K, Naya Y, Ichikawa T, Seki N. 2018. Regulation of antitumor miR-144-5p targets oncogenes: direct regulation of syndecan-3 and its clinical significance. *Cancer Science* **109**:2919–2936 DOI 10.1111/cas.13722.

Yang C, Wang Z, Li L, Zhang Z, Jin X, Wu P, Sun S, Pan J, Su K, Jia F, Zhang L, Wang H, Yu X, Shao X, Wang K, Qiu F, Yan J, Huang J. 2021. Aged neutrophils form mitochondria-dependent vital NETs to promote breast cancer lung metastasis. *The Journal for ImmunoTherapy of Cancer* **9**(10):e002875 DOI 10.1136/jitc-2021-002875.

Yao Z, Zheng X, Lu S, He Z, Miao Y, Huang H, Chu X, Cai C, Zou F. 2019. Knockdown of FAM64A suppresses proliferation and migration of breast cancer cells. *Breast Cancer* **26**:835–845 DOI 10.1007/s12282-019-00991-2.

Yu G, Wang LG, Han Y, He QY. 2012. clusterProfiler: an R package for comparing biological themes among gene clusters. *Omics* **16**:284–287 DOI 10.1089/omi.2011.0118.

Zhang H, Dai Z, Wu W, Wang Z, Zhang N, Zhang L, Zeng WJ, Liu Z, Cheng Q. 2021. Regulatory mechanisms of immune checkpoints PD-L1 and CTLA-4 in cancer. *Journal of Experimental & Clinical Cancer Research* **40**:184 DOI 10.1186/s13046-021-01987-7.

Zhang J, Qian L, Wu J, Lu D, Yuan H, Li W, Ying X, Hu S. 2019. Up-regulation of FAM64A promotes epithelial-to-mesenchymal transition and enhances stemness features in breast cancer cells. *Biochemical and Biophysical Research Communications* **513**:472–478 DOI 10.1016/j.bbrc.2019.03.207.

Zhao WM, Coppinger JA, Seki A, Cheng XL, Yates 3rd JR, Fang G. 2008. RCS1, a substrate of APC/C, controls the metaphase to anaphase transition. *Proceedings of the National Academy of Sciences of the United States of America* **105**:13415–13420 DOI 10.1073/pnas.0709227105.

Zhong L, Yang Z, Lei D, Li L, Song S, Cao D, Liu Y. 2021. Bromodomain 4 is a potent prognostic marker associated with immune cell infiltration in breast cancer. *Basic & Clinical Pharmacology & Toxicology* **128**:169–182 DOI 10.1111/bcpt.13481.

Zhou T, Cai Z, Ma N, Xie W, Gao C, Huang M, Bai Y, Ni Y, Tang Y. 2020. A novel ten-gene signature predicting prognosis in hepatocellular carcinoma. *Frontiers in Cell and Developmental Biology* **8**:629 DOI 10.3389/fcell.2020.00629.

Zhou Y, Ou L, Xu J, Yuan H, Luo J, Shi B, Li X, Yang S, Wang Y. 2021. FAM64A is an androgen receptor-regulated feedback tumor promoter in prostate cancer. *Cell Death & Disease* **12**:668 DOI 10.1038/s41419-021-03933-z.

Zhu H, Hu X, Feng S, Jian Z, Xu X, Gu L, Xiong X. 2022. The hypoxia-related gene COL5A1 is a prognostic and immunological biomarker for multiple human tumors. *Oxidative Medicine and Cellular Longevity* **2022**:6419695 DOI 10.1155/2022/6419695.

Zhu H, Hu X, Ye Y, Jian Z, Zhong Y, Gu L, Xiong X. 2021. Pan-cancer analysis of PIMREG as a biomarker for the prognostic and immunological role. *Frontiers in Genetics* **12**:687778 DOI 10.3389/fgene.2021.687778.